การเฝ้าสังเกตการแกว่งของกำลังไฟฟ้าระหว่างพื้นที่แบบเวลาจริงโดยใช้อุปกรณ์วัดแบบเฟสเซอร์

นายอัสนิ รอยส์ อลิ

วิทยานิพนธ์นี้เป็นส่วนหนึ่งของการศึกษาตามหลักสูตรปริญญาวิศวกรรมศาสตรมหาบัณฑิต
สาขาวิชาวิศวกรรมไฟฟ้า ภาควิชาวิศวกรรมไฟฟ้า
คณะวิศวกรรมศาสตร์ จุฬาลงกรณ์มหาวิทยาลัย
ปีการศึกษา 2555

REAL-TIME MONITORING OF INTER-AREA POWER OSCILLATION
USING PHASOR MEASUREMENT UNITS

Mr. Husni Rois Ali

A Thesis Submitted in Partial Fulfillment of the Requirements
for the Degree of Master of Engineering Program in Electrical Engineering
Department of Electrical Engineering
Faculty of Engineering
Chulalongkorn University
Academic Year 2012

Thesis Title   REAL-TIME MONITORING OF INTER-AREA POWER OSCILLATION USING PHASOR MEASUREMENT UNITS

By   Mr. Husni Rois Ali

Field of Study   Electrical Engineering

Thesis Advisor   Assistant Professor Naebboon Hoonchareon, Ph.D.

Accepted by the Faculty of Engineering, Chulalongkorn University in Partial Fulfillment of the Requirements for the Master's Degree

.... Dean of the Faculty of Engineering

(Associate Professor Boonsom Lerdhirunwong, Dr. Ing.)

THESIS COMMITTEE

.... Chairman

(Professor David Banjerdpongchai, Ph.D.)

.... Thesis Advisor

(Assistant Professor Naebboon Hoonchareon, Ph.D.)

.... Examiner

(Assistant Professor Kulyos Audomvongseree, Ph.D.)

.... External Examiner

(Associate Professor Issarachai Ngamroo, Ph.D.)

อัสนิ รอยส์ อลิ: การเฝ้าสังเกตการแกว่งของกำลังไฟฟ้าระหว่างพื้นที่แบบเวลาจริงโดยใช้ อุปกรณ์วัดแบบเฟสเซอร์. (REAL-TIME MONITORING OF INTER-AREA POWER OSCILLATION USING PHASOR MEASUREMENT UNITS) อ. ที่ปรึกษาวิทยานิพนธ์หลัก: ผศ.ดร. แนบบุญ หุนเจริญ, 73 หน้า.

ปัญหาเสถียรภาพเชิงการแกว่งของกำลังไฟฟ้าระหว่างพื้นที่ อาจเป็นสาเหตุทำให้เกิดปัญหา ไฟฟ้าดับในวงกว้าง   ด้วยภาวะการทำงานของระบบไฟฟ้าเปลี่ยนแปลงอย่างต่อเนื่องทำให้ปัญหา เสถียรภาพดังกล่าว ยากแก่การสังเกตุ เครื่องมือในการเฝ้าสังเกตการแกว่งของกำลังไฟฟ้าระหว่างพื้นที่ แบบเวลาจริงจะมีส่วนสำคัญในการรักษาเสถียรภาพของระบบไฟฟ้า วิทยานิพนธ์นี้นำเสนอระบบเฝ้า สังเกตการแกว่งของกำลังไฟฟ้าระหว่างพื้นที่แบบเวลาจริงโดยระบุความถี่การแกว่ง รวมถึงความหน่วง ความสัมพันธ์ระหว่างโหมดกับตัวแปรที่เกี่ยวข้อง การระบุคุณสมบัติการแกว่งอาศัยข้อมูลจากอุปกรณ์ วัดแบบเฟสเซอร์ โดยประยุกต์เทคนิคการลดแนวโน้ม และการลดอัตราสุ่มในการประมวลผลข้อมูล เบื้องต้น ขั้นตอนวิธีของโมดิฟายยูวอคเกอร์ถูกใช้ในการระบุโหมดความถี่และโหมดความหน่วง แล้วใช้ การพิจารณาพาวเวอร์สเปกตรัมเดนซิตี ร่วมกับครอสสเปกตรัมเดนซิตี ในการระบุความสัมพันธ์ของตัว แปรในโหมดดังกล่าว นอกจากนี้การเฝ้าสังเกตุแบบเวลาจริงยังมีตัวเลือกข้อเสนอแนะสำหรับผู้ ปฏิบัติการเพื่อเพิ่มสมรรถนะการหน่วงการแกว่ง ข้อเสนอแนะกำหนดโดยหลักการวิเคราะห์ความไวเชิง โหมด ผลลัพธ์ถูกแสดงบนส่วนต่อประสานผู้ใช้ ระบบไฟฟ้าอย่างง่ายที่ประกอบด้วยเครื่องกำเนิดไฟฟ้า 17 ชุดในอเมริกาตะวันตกเฉียงเหนือถูกใช้เป็นระบบทดสอบ ผลลัพธ์แสดงให้เห็นว่าเครื่องมือเฝ้าระวัง แบบเวลาจริงที่นำเสนอสามารถตรวจจับการแกว่งของกำลังไฟฟ้าระหว่างพื้นที่ได้อย่างแม่นยำ และ สามารถให้คำแนะนำเพื่อปรับปรุงความหน่วงของระบบไฟฟ้ากำลังได้ ขั้นตอนวิธีนี้สามารถทำงานได้ดี ทั้งในเงื่อนไขการทำงานปกติและในภาวะถูกรบกวนของระบบไฟฟ้ากำลัง

ภาควิชา	วิศวกรรมไฟฟ้า	ลายมือชื่อนิสิต	
สาขาวิชา	วิศวกรรมไฟฟ้า	ลายมือชื่อ อ.ที่ปรึกษาวิทยานิพนธ์หลัก	
ปีการศึกษา	2555		

5470519721 : MAJOR ELECTRICAL ENGINEERING

KEYWORDS : INTER-AREA POWER OSCILLATION / PHASOR MEASUREMENT UNIT / REAL-TIME MONITORING / SYSTEM IDENTIFICATION

HUSNI ROIS ALI : REAL-TIME MONITORING OF INTER-AREA POWER OSCILLATION USING PHASOR MEASUREMENT UNITS. ADVISOR : ASST. PROF. NAEBBOON HOONCHAREON, Ph.D., 73 pp.

The stability problem of inter-area power oscillation may cause system blackout. Due to continuously changing of power system operating condition, it makes such stability problem difficult to observe. Real-time monitoring of inter-area power oscillation will play an important role in maintaining the power system stability. This thesis proposes real-time monitoring system of inter-area power oscillation stability by identifying predominant modes of oscillation as well as the associated mode damping and mode shape. The identification process is based on PMU data with preprocessing technique consisting of detrending and downsampling. The Modified Yule-Walker (MYW) algorithm is utilized for identifying frequency of oscillation and mode damping while combined Power Spectral Density (PSD) and Cross Spectral Density (CSD) are used for mode shape identification. In addition, the real-time monitoring system is equipped with operational recommendation options to provide the operator with guidelines to improve Power Oscillation Damping (POD). The recommendation is established based on the concept of mode sensitivity analysis. These identification results are then displayed on GUI to assist the power system operator to monitor system condition in real-time. The simplified 17-machine Western North American power grid system is used to verify the monitoring system performance. The results show that the proposed real-time monitoring system is able to accurately track the predominant modes of oscillation as well as to provide the system operator with recommendation for to improve power system damping. The real-time monitoring system works well during both ambient and ringdown conditions.

Department : ....Electrical Engineering....   Student's Signature ....

Field of Study : ....Electrical Engineering....   Advisor's Signature ....

Academic Year : ....2012...........

Acknowledgements

First of all, I would like to express my gratitude to my supervisor Assistant Professor Naebboon Honchareon for careful guidance and constant support during my study. It gives me a huge pleasure and experience to work with him. This thesis would not have been completed without his great courage and supervision.

I greatly appreciate formidable effort and valuable comment of my committee member including Professor David Banjerdpongchai, Assistant Professor Kulyos Audomvongseree, and Associate Professor Issarachai Ngamroo. I would like also to express gratitude to all Professors at Department of Electrical Engineering, Chulalongkorn Univerity for providing me valuable knowledge and useful background about the power system and control. My thanks also to all member of Power System Research Laboratory (PSLR) for tremendous help and fruitful discussion. Special appreciation also goes to Prof Dan Trudnowski at Montana Tech and Prof Joe Chow at Rensselaer Polytechnic Institute for their generosity to provide me detail of their work.

I would like also to express my gratitude to my beloved parent: Hamtoyo and Nur Widayati, my beloved brother: Ibnu Farhatani,my beloved sister: Putri Alya Wulandari, my parent in law: Slamet Suripto and Lina Pariatin, and to all members of my family: my grandparents: Mr./Mrs. Mudo Sihono, Mr./Mrs. Muh Giyanto, my uncle: Mr. Zuhud, my auntie: Mrs. Silah and family, and every one whom I am unable mention them one by one. It is because of their endless pray, finally I can accomplish this work. My most profound acknowledgment must go to my wife, Anisah, for her endless patient, love, and support.

Lastly, I would like to express my foremost gratitude to ALLAH for giving me Islam as the way of my life. There is no power and strength except with ALLAH.

Contents

List of Tables

List of Figures

CHAPTER I

INTRODUCTION

1.1 Motivation

Power system today is increasing in size. The operation of power system thus becomes much more complex than it used to be in the past. Moreover, due to many constrains such as economic constraints and environmental constraints, power system is pushed to operate near its limit. As a result, the ability of power system in maintaining stable operation points is a crucial factor.

One of the main problems of power system today is inter-area oscillation stability problem. The Inter-area stability is a sub-class of small signal stability. It is the phenomenon of oscillation among areas in power system [1], [2]. The problem is caused by the lack of available damping in power system.

In order to analyze small signal stability problem in common and inter-area oscillation in particular, the most commonly used method is by linearizing power system equations around operating point and finding corresponding eigen properties of the system. This method is normally termed as modal analysis [2], [3]. However, the eigen properties method can only be applied to small size system. Eigen properties consisting of frequency and damping of oscillation modes and mode shape give complete information about the oscillation behavior in power system. To be applied in real power system, the methods is not feasible since it is difficult to set up the equation governing the real system. Even if one can construct the complete power system mathematical model, the solution to find the eigen properties is often time consuming. As a result, this method cannot be used for monitoring purposes since in monitoring, the computation time should be reasonably fast.

Another method to analyze small signal stability problem in power system is by using measurement based method [4], [5], [6], [7]. Measurement based method relies on the system identification tools and signal processing analysis in order to estimate reduced order model of the system. It is based on the measurement of power system variables such as frequency [8], voltage (V), voltage angle (θ), current (I), and current angle (ϕ) [9]. The method can provide the reduced power system model very fast without having to know the real power system model. Thus the measurement based method is promising to be deployed in online monitoring of power system small signal stability. The Process to analyze small signal stability problem can be briefly describe in the Figure 1.1.

The measurement based method now becomes more powerful due to the advent of Phasor Measurement Unit (PMU) [10]. The PMU can provide very accurate data due to its ability to be synchronized with GPSs clock. The accurate data makes the system identification result very accurate. The PMU can also sample the data very fast.
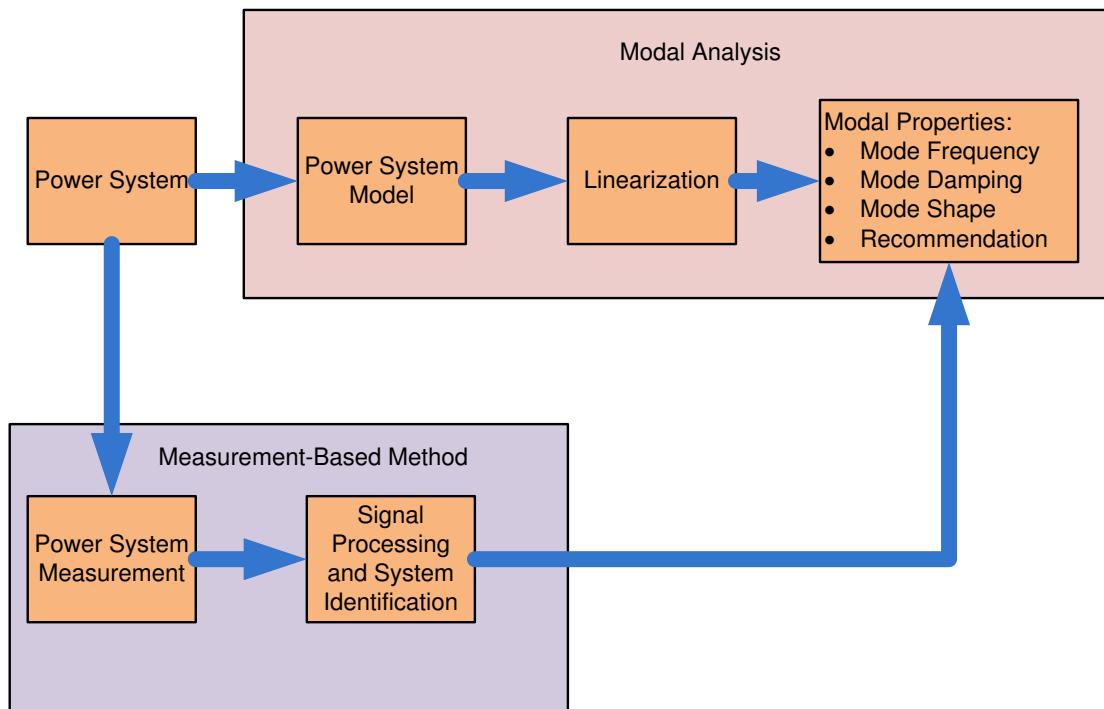
Figure 1.1: Modal analysis vs measurement-based method

For real-time application, the fast analyzing time is not the only determining factor. There are some other factors need to be taken into account.The identification result should be accurate enough to provide correct information of the system condition. The Reliability of the estimation also must be considered. In real-time application, there are disturbances that can excite power system, and in this condition the identification should not fail because of this factor.

Since the measurement based method normally relies on PMU, the compatibility with existing monitoring system must be established. In many power systems, the SCADA system as an example has been widely used. The measurement-based method system must deteriorate performance of the existing monitoring system. Another important factor which now people are interested in is that the result of identification should include the recommendation action for the system operator. Recommendation action is important to prevent system black out when the system stability condition is weak. Recommendation action gives the list of action to improve system stability condition.

All of these factors must be consider in order to build application for monitoring small signal stability of the power system.

1.2 Specific Objectives

This research aims to develop the application program for monitoring inter-area power oscillation using Phasor Measurement Unit. This includes:

- Identifying mode frequency and mode damping of inter-area power oscillation.

- Identifying the mode shape of oscillation.

- Providing recommendation action to the operator to improve stability condition.

- Building Graphical User Interface (GUI).

1.3   Scope of Work

Scope of work of this thesis are:

1. Focus on inter-area oscillation.

2. The simplified Western North American power system (WNAPS) 17 machine system [11] is used to test the performance of the monitoring system.

3. Load is represented as random low-pass filtered Gaussian White Noise ($1/f$ filter). This random load model is hypothesized sufficient for load [12].

4. This work is to estimate:

   - Mode frequency and mode damping of inter-area power oscillation.

   - Mode shape of the oscillation.

   - Recommendation action to system operator.

5. The identification results are compared to modal analysis's results to check the accuracy.

6. To develop GUI for real-time monitoring.

7. Communication noise and delay are neglected.

1.4   Methodology

1. Literatur survey on:

   - Small signal stability analysis.

   - Phasor Measurement Unit (PMU).

   - Modal Properties identification i.e. mode frequency, mode damping, and mode shape identification.

   - Modal sensitivity identification.

   - PMU application for inter-area power oscillation monitoring.

2. Determine the specific objective and scope of work.

3. Formulate the problem.

4. Determine the solution method.

5. Build and test the power system model and real-time monitoring.

6. Analyze and conclude the result.

1.5   Expected Contributions

Due to the large size of power system today, operator often finds the difficulties to monitor the condition of power system especially the stability of inter area oscillations. The system condition keeps changing due to continuously changing of load, generation, fault, and so on. As a result, operator often does not realize that the power system almost approaches or even has entered the instability conditions. The presence of monitoring system is able to assist the operator monitor the power system condition and also increase the observability of power system state. This research aim to build an interactive GUI monitoring system based on PMU measurement to assist the operator monitor system condition and to provide various information about inter-area oscillation. The information displayed in the GUI includes frequency, damping, and mode shape of the oscillation. This monitoring system can also provide the recommendation action to the operator for improving Power Oscillation Damping (POD).

CHAPTER II

SMALL SIGNAL STABILITY

2.1   Introduction

Small signal stability is classified as a class of power system stability. Power system stability is defined as characteristic for a power system to remain in a state of equilibrium at normal operating conditions and to restore an acceptable state of equilibrium after a disturbance [3]. From the definition, one can intuitively imply that small signal stability deals only with small signal disturbances. The complete classification of power system stability is presented in the Figure 2.1 [3]. It can be seen that small signal stability can show up as non-oscillatory instability and oscillatory instability. Non-oscillatory stability is caused by the insufficient synchronizing torque thus it makes the system is out-of-step. When this condition occur, the system may no longer be able to maintain the synchronous operation.

On the other hand, the oscillatory stability is caused by the insufficient damping in the power system. The oscillatory stability has unique appearance in which there will be persisting swing oscillations before the instability occurs. This instability is further divided into local plant modes, inter-area modes, control modes, and torsional modes. Control modes is strongly associated by incorrectly tuning of control apparatus of power system such as governor, SVC, and exciter. While, torsional modes normally oscillates with frequency range 10 to 46 Hz. It is related to generator turbine system. The problem often occurs in tandem turbine [13]. Local plant modes is the oscillation one generation system swings against the rest of the system. Normally, it ranges between 0.7 to 2.0 Hz [1]. In analyzing local modes, Normally the rest of system is represented as single machines and this system is well-known as single machine infinite bus (SMIB) [14].

Meanwhile, the inter-area modes is involved one group of generator swinging against another group of generator. The oscillation usually lies from 0.1 to 0.8 Hz [1]. The effect of this instability can be seen over wide system range. As a result, when it occurs, the effect is much more significance than other modes instability. The inter-area mode normally occurs when one area of power system is connected to another area using weak transmission lines. The oscillation becomes more apparent as the loading of the transmission lines increase. Since it involves low frequency oscillation and wider system range, the inter-area modes is much more difficult to analyze and consequently much more difficult to cope [1]. Power system stabilizers (PSS) is often deployed in the system to resolve inter-area oscillation problem. Among oscillatory instability classes, perhaps the inter-area modes is the most important one.

There are a lot of reports discussing about the occurrence of inter-area problem in the past [14].
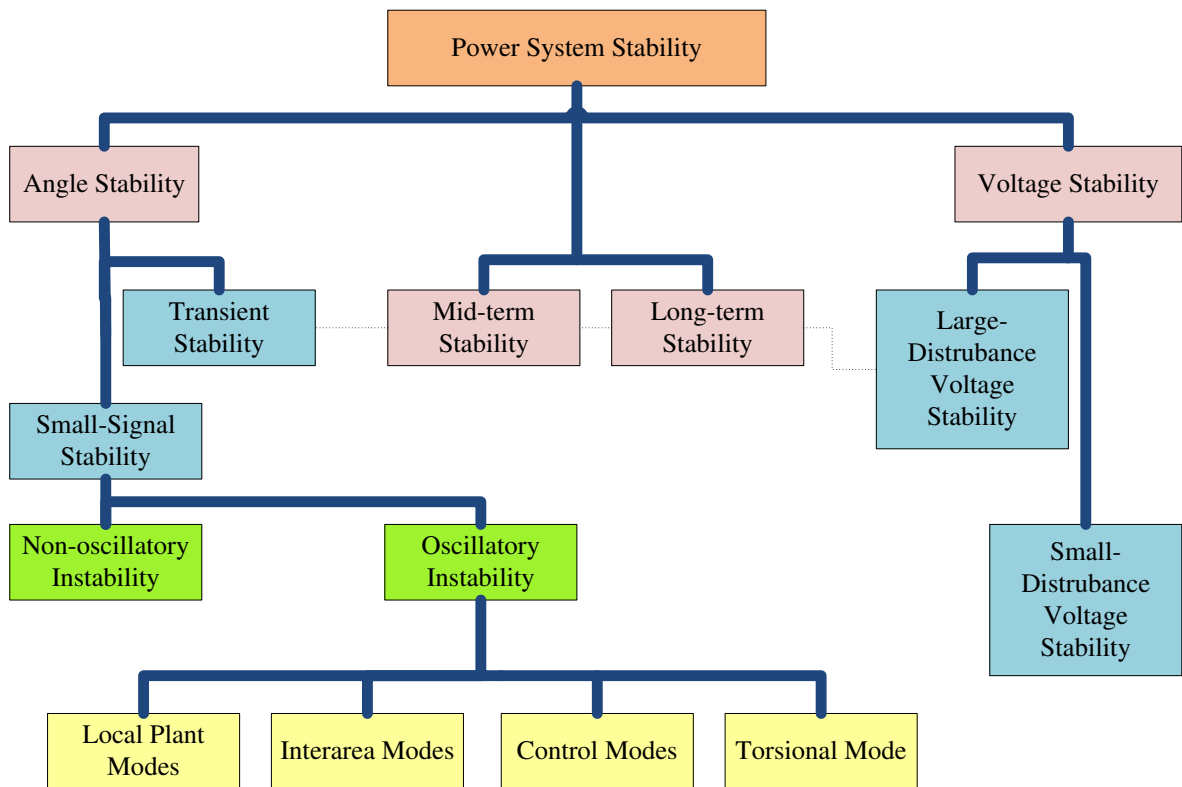
Figure 2.1: Power system stability classification

One of the most prominent one is the 1996 break up which made major system break up in Western North America Power System (WNAPS). The chronological order of the system break up can be seen in the Figure 2.2 [15].

2.2 Modal Analysis

Modal analysis has been a standard for analyzing small signal stability of power system. There are many excellent references related to this subject [2, 3, 8]. The basic assumption in modal analysis is that under small perturbation any system, including power system, can be described by linear equation as shown by equation (2.1)

$$\underline{\dot{x}}(t) = A\underline{x}(t) + B\underline{q}(t) \tag{2.1}$$

This equation is termed as state-space equation. $\underline{x}$ is state vector, A and B are Jacobian matrices and $\underline{q}(t)$ is the input. The system in equation (2.1) has eigenvalues and eigenvector which can be calculated using equation (2.2)–(2.4)

$$|\lambda_i I - A| = 0 \tag{2.2}$$

$$A\underline{u}_i = \lambda_i \underline{u}_i \tag{2.3}$$

$$\underline{v}_i A = \lambda_i \underline{v}_i \tag{2.4}$$
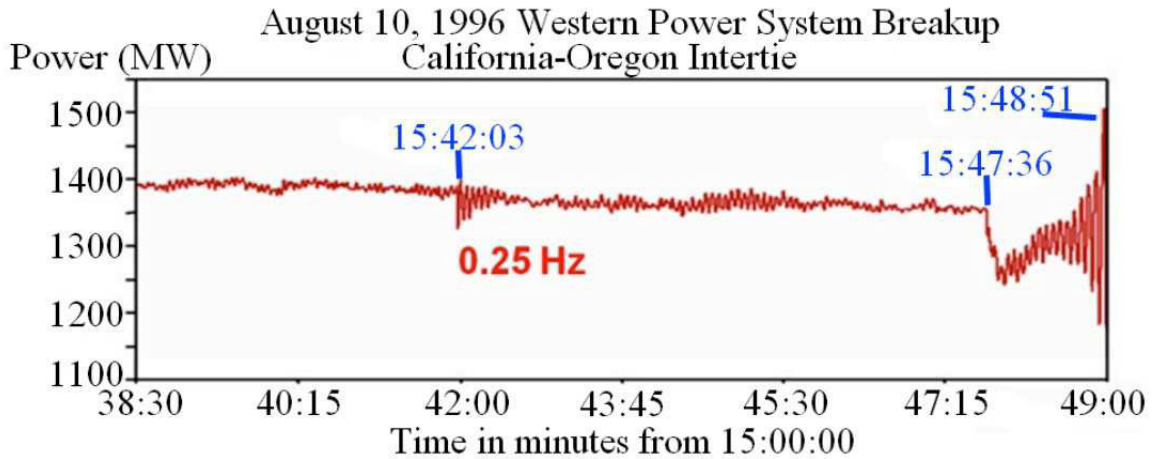
Figure 2.2: Power flow during North America system break up in 1996

where $\lambda_i = \alpha_i + j\omega_i$ denotes the ith eigenvalue while i^{th} and $\underline{v}_i$ are the ith right and left eigenvector respectively. The mode frequency and mode damping of λ_i can be obtained using equation (2.5) and (2.6)

$$f_i = \frac{\omega_i}{2\pi} \tag{2.5}$$

$$\zeta_i = \frac{-\alpha}{\sqrt{\alpha^2 + \omega_i^2}} \tag{2.6}$$

The system is stable if all α_i lie on the left half plane of s-plane. This is equivalent to all α_i have positive damping ζ_i.

Two nxn matrices can be formed using each single right and left eigenvector element

$$U = [\underline{u} \cdots \underline{u}_i] \tag{2.7}$$

$$V = [\underline{v}^T \cdots \underline{v}_i^T] \tag{2.8}$$

U and V are orthonormal matrices with property $VU = I$.

Equation (2.1) can be diagonalize by first defining linear transformation

$$z_i(t) = \underline{v}_i \underline{x}(t) \tag{2.9}$$

applying this transformation to equation (2.1) and it will result

$$\dot{\underline{z}}(t) = \lambda_i z_i(t) + \underline{v}_i B \underline{q}(t) \tag{2.10}$$

using equation (2.9) each state can be expressed using

$$\underline{x}(t) = \sum_{i=1}^{n} z_i(t) \underline{u}_i \tag{2.11}$$

Equation (2.11) gives the information about the activity modes in a particular state. The amplitude $u_{i,k}$ provides the magnitude of mode z_i in state x_k thus it gives the observability of mode in

state. The angle $u_{i,k}$ provides about the phasing of mode z_i in state x_k. The $u_{i,k}$ is termed as mode shape [2, 3, 8].

In small signal stability study, mode frequency, mode damping and mode shape share very important information about the system stability. They inform about the stability condition in the system as well as the states related to the stability.

2.3 Modal Sensitivity

Modal sensitivity informs how the modal properties i.e mode frequency, mode damping, and mode shape change as operating parameters such as generator loading, transmission loading, or control parameters changes as well. There are many previous study utilizing modal sensitivity to select proper location of PSS [16] and FACTS devices [17]. Modal sensitivity can also be used to obtain recommendation action to the operator.

In order to calculate modal sensitivity, one may start from equation (2.3) [3] i.e.

$$A\underline{u}_i = \lambda_i \underline{u}_i$$

by differentiating with respect to a_{kj} i.e element of A in k^{th} row and j^{th} column, it can be obtained

$$\frac{\partial A}{\partial a_{kj}}\underline{u}_i + A\frac{\partial \underline{u}_i}{\partial a_{kj}} = \frac{\partial \lambda_i}{\partial a_{kj}}\underline{u}_i + \lambda_i\frac{\partial \underline{u}_i}{\partial a_{kj}} \tag{2.12}$$

premultiplying by $\underline{v}_i$, it will result

$$\underline{v}_i\frac{\partial A}{\partial a_{kj}}\underline{u}_i = \frac{\partial \lambda_i}{\partial a_{kj}} \tag{2.13}$$

by recalling that $\underline{v}_i\underline{u}_i$=1 and $\underline{v}_i(A - \lambda_i I)$=0

Although the equation (2.13) is specific case of differentiating with respect to a_{kj}, one can extend the equation (2.13) into more general form [18]

$$\underline{v}_i\frac{\partial A}{\partial p}\underline{u}_i = \frac{\partial \lambda_i}{\partial p} \tag{2.14}$$

p denotes any operating parameters interest such as transmission loading, generation loading, and load. For small signal perturbation, the equation (2.14) can be approximated by

$$\underline{v}_i\frac{\Delta A}{\Delta p}\underline{u}_i = \frac{\partial \lambda_i}{\partial p} \tag{2.15}$$

using the equation (2.15), it can be obtained the sensitivity of operating parameters to the mode change.

CHAPTER III

POWER SYSTEM OSCILLATION IDENTIFICATION

3.1 Dynamic System Representation

As being explained in chapter 2, the basic assumption in small signal stability analysis is that the power system is perturbed by small disturbances. This assumption allows power system to be described by linear equation (2.1).

For system identification purposes, equation (2.1) can be extended into generalized equation [19]

$$\dot{\underline{x}}(t) = A\underline{x}(t) + B_L\underline{q}(t) + B_E\underline{u}_E(t) \tag{3.1}$$

$$y(t) = C\underline{x}(t) + D_L\underline{q}(t) + D_E\underline{u}_E(t) + \mu(t)$$

Where $\underline{q}$ is a hypothetical random vector perturbing the system, $\underline{u}_E$ is the exogenous input such as load pulse, low-level probing signal and μ is measurement noise and $\dot{\underline{x}}$ denotes system states. While y contains system outputs.

The system in equation (3.1) can be represented in block diagram shown in the Figure 3.1. The y_i is the i$^{\text{th}}$ system output y. When trying to measure the y_i, normally the noise μ_i is added to the measurement. Thus the true measured signal is y_i. K and $K\prime$ represent deliberate and not deliberate topology change respectively. It can be done by closing switch s and $s\prime$. The topology change will produce ringdown output showing up in the output y_i. Ringdown signal is characterized by big oscillation in y_i. Ringdown signal is also produced when the sudden input is inserted by $\underline{u}_E$.

Meanwhile, the input $\underline{q}$ normally behaves randomly. In real power system, it is similar to small random load changing. As a result of this perturbation, the ambient data will be produced in the output y_i. Ambient data is characterized by random small fluctuation in y_i. In many cases, the operator can also intentionally insert random input $\underline{u}_E$. This injection is usually carried out for improving the identification result.

3.2 Identification Techniques

The basic principle of system identification is to estimate the system G using measured data y_i and measured input $\underline{u}_E$. However in most cases of power system, one can only measure the system output y_i since the input $\underline{q}$ is unknown. It is similar to real power system that one cannot measure the random load changing at every single load.

Therefore, it is obvious that the knowledge of data will significantly affect the system identification process. Normally, the system identification in power system is classified based on the data
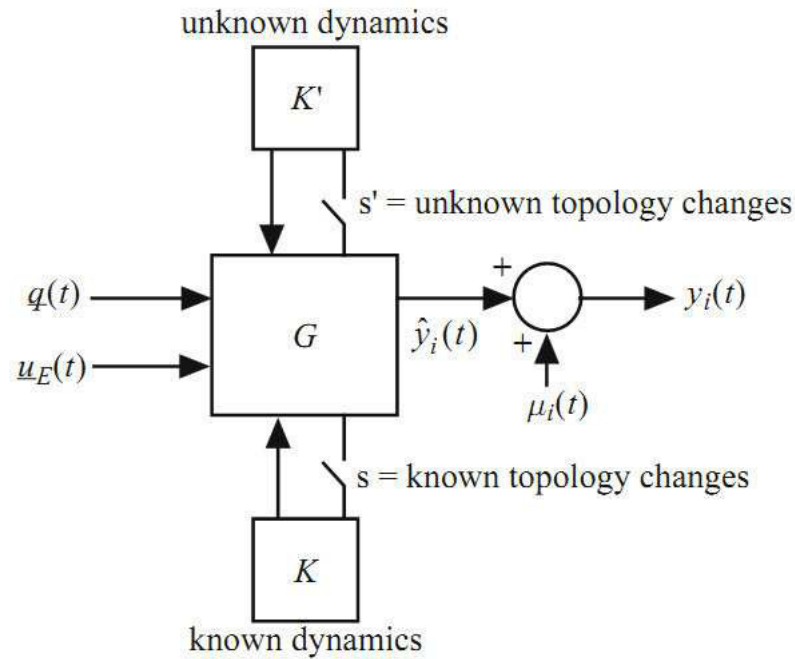
Figure 3.1: System structure for system identification

type. Zhou., N., et all [7] classify the system identification similar to what is shown in the Figure
3.2. The data from PMU measurement can be divided into non-typical data and typical data. Non-
typical data cannot be used for identification purposes since it is not produced by the system. The
presence of non-typical data will degrade the result of system identification. There are a lot example
of non-typical data such as measurement device malfunction, lost data, outliers, and noise.

On the other hand, typical the data is data that can be used for identifying the system. The
data is produced by the dynamic of the system thus it represents the dynamic behavior of the system.
Ringdown data and ambient data are examples of typical data. As being mentioned in the subsection
3.1, the ringdown data is produced by large disturbance such as temporary fault and it can be seen to
have strong system oscillation response. Ringdown data needs ringdown algorithm for identification.
There are many publications reporting ringdown techniques such as Prony analysis [20], [21], the
Eigenvalue Realization Algorithm (ERA) [22], the matrix pencil method [23] and the Hankel total
least squares (HTLS) [23]. Among these methods, Prony analysis is the most widely used analysis.
In analyzing ringdown data, the data length requirement is normally around 5–20 s since ringdown
data contains very rich information about system characteristic. Therefore, it is unnecessary to use
very long data window.

While the ringdown data is characterized by large disturbance, ambient data is produced by
random input such as random load changing power system. Normally, data requirement is much
longer than that of ringdown data. Data length requirement is usually in order minutes. Ambient data
can be analyzed by several methods such as YuleWalker (YW) algorithm [24], modified YW method
for ARMA model [25], CVA (canonical variate algorithm) [26], N4SID (Numerical algorithm for
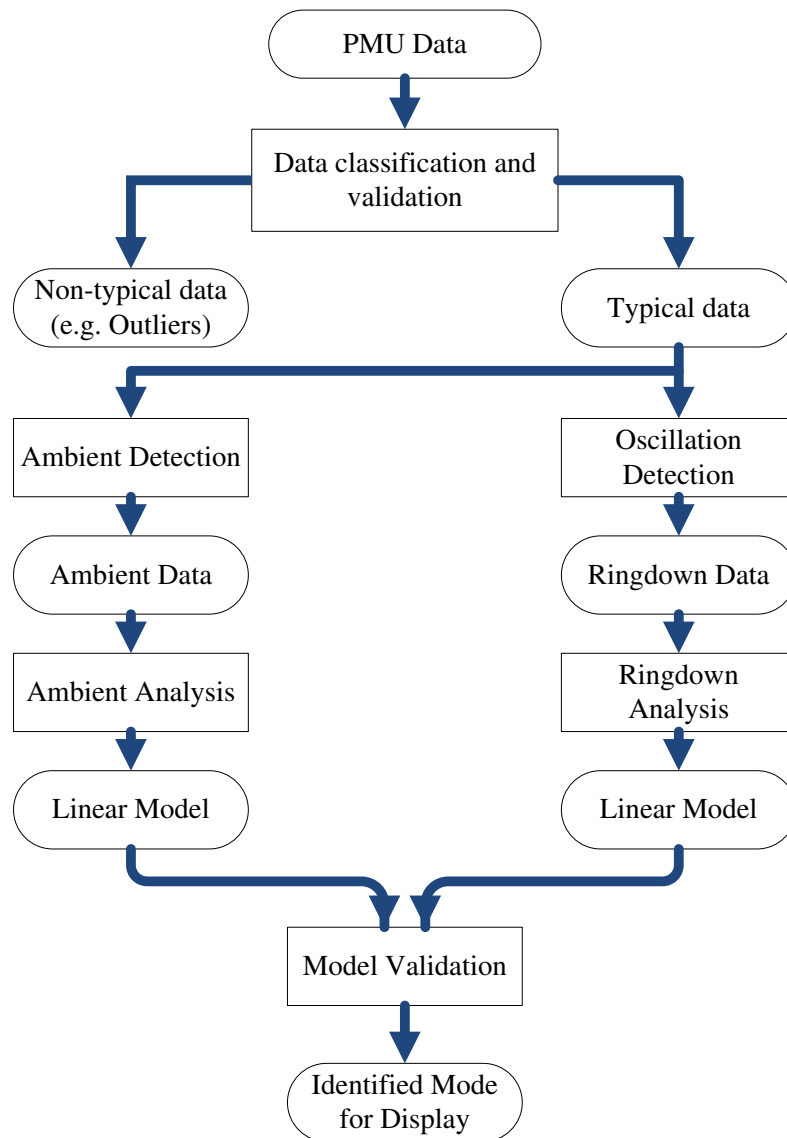
Figure 3.2: PMU data classification

subspace statespace system identification) [4], YuleWalker Spectrum (YWS) [19], and Frequency-Domain Decomposition (FDD) [27].

Beside those two types of algorithms, there is also an algorithm working for both ringdown data and ambient data. This is called mode-meter algorithm. The regularized robust recursive least-squares (R3LS) [5], [6] method is an example of mode-meter algorithm.

3.3 Mode Frequency and Mode Damping Identification

In this research, to identify mode frequency and mode damping of inter-area power oscillation, the Modified Yule-Walker method (MYW) [25] is used. MYW assumes that the system is perturbed by random load changing which is the typical case in real power system. The method does not require a big oscillation in the identification process.
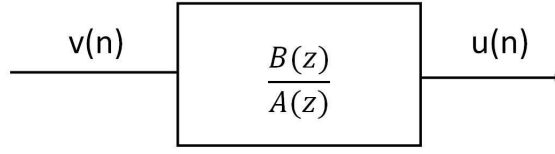
Figure 3.3: ARMA model with white-noise input

The system is modeled as ARMA model structure shown in Figure 3.3. For the model in Figure 3.3, the corresponding difference equations is

$$u(n) + a_1 u(n-1) + \cdots + a_N u(n-N)$$
$$= b_0 v(n) + b_1 v(n-1) + \cdots + b_M v(n-M)$$

(3.2)

Where $a_1, \cdots, a_N$ and $b_1, \cdots, b_M$ are the coefficient for characteristic equation of poles and zeros respectively. It is assumed that the system is driven by Gaussian white noise $v(n)$.

The AR parameters can be calculated from covariance of the data, $r(k) = Eu(n)u(n-k)$. It can be carried out by multiplying both sides of difference equations by $u(n-k)$, and it gives

$$r(k) = \sum_{i=1}^{N} a_i r(k-i) = \sum_{j=0}^{M} b_j Ev(n-j)u(n-k)$$

(3.3)

For $k > m$, the output is uncorrelated with future input. Thus, the expectation will be zero, and the right side is zero. Equation (3.3) above is then simplified to

$$r(k) + \sum_{i=1}^{N} a_i r(k-i) = 0$$
$$\text{for } k > M$$

(3.4)

The expression in equation (3.4) can be expanded for $k = M+1, M+2, \cdots M+P$ in matrix equation

$$-\underline{r} = R\underline{a}$$

(3.5)

where

$$\underline{r} = [r(M+1)\ r(M+2) \cdots r(M+P)]^T$$

$$R = \begin{bmatrix} r(M) & r(M-1) & \cdots & r(M-N+1) \\ r(M+1) & r(M) & \cdots & r(M-N+2) \\ \vdots & \vdots & \ddots & \vdots \\ r(M+P-1) & r(M+P) & \cdots & r(M-N+P) \end{bmatrix}$$

and

$$\underline{a} = [a_1\ a_2 \cdots a_N]^T$$

P represents the number of equations being used in determining AR coefficient.

In real application, the real values of autocorrelation are unknown therefore it can be estimated from sample data by equation (3.6)

$$\hat{r}(k) = \frac{1}{N} \sum_{n=k}^{N-1} u(n)u(n-k) \tag{3.6}$$

The matrix equation in equation (3.5) is usually over determined which is well-known as Modified Yule-Walker method. The optimal number of equation used, P, is unknown. However if $P > N$, the AR coefficients can be calculated in least square sense.

Once the AR coefficients are calculated, the poles of the estimated system can be determined by finding the roots of characteristic equation. These poles are in z-domain. In order to find the poles in the corresponding s-domain, one can use equation (3.7)

$$s_i = \frac{\ln(Z_i)}{T} \tag{3.7}$$
$$i = 1, 2, \cdots, N$$

It is often the case that the true order of the system (n) is unknown therefore for identification purpose the large value of n is normally selected. As a result, there will be several artificial modes besides the estimates modes. The problem is to choose which modes are dominant. This process is called mode selection [19]. The mode selection is based on the concept of "pseudo energy" of a given mode within an autocorrelation function. If equation 3.8 is transformed using Z-transform

$$r_i q(k) = -\sum_{j=1}^{n} a_j r_i(q-j), q > m \tag{3.8}$$

and solve for in parallel form, one can obtain

$$r_i q(k) = -\sum_{j=1}^{n} B_{ij} z_j^{q-m-1}, q > m \tag{3.9}$$

Where z_j is the j$^{\text{th}}$ discrete pole and B_{ij} is the residual of pole z_i and output i. One can expand equation 3.9 into matrix form

$$\begin{bmatrix} z_1^0 & z_2^0 & \cdots & z_n^0 \\ z_1^1 & z_2^1 & \cdots & z_n^1 \\ \vdots & \vdots & \ddots & \vdots \\ z_1^{M-1} & z_2^{M-1} & \cdots & z_n^{M-1} \end{bmatrix} \begin{bmatrix} B_{i1} \\ B_{i2} \\ \vdots \\ B_{in} \end{bmatrix} = \begin{bmatrix} R_i(m+1) \\ R_i(m+2) \\ \vdots \\ R_i(m+M) \end{bmatrix} \tag{3.10}$$

The coefficients B_{ij} can be obtained in least square sense. The pseudo energy of mode j is

$$E_j = \sum_{i=1}^{n_0} \left(B_{ij}^* B_{ij} \sum_{q=0}^{M-1} \left[(Z_j^q)^* (Z_j^q) \right] \right) \tag{3.11}$$

Once all E_j are calculated, modes are sorted based on the magnitude E_j. The last step is to choose the mode within specific region of s-plane. Normally, the modes having low damping within inter-area frequency ranges are selected.

3.4   Mode Shape Identification

The main task of mode shape identification is to obtain $\underline{u}_i$ from measurement signal. it can be achieved using spectral analysis. The derivation here follows the concepts in [8]. Two spectral functions are defined first

$$S_{kl}(\omega) = \lim_{T\to\infty} \frac{1}{T} E\{Y_k^*(\omega)Y_l(\omega)\} \tag{3.12}$$

$$S_{kk}(\omega) = \lim_{T\to\infty} \frac{1}{T} E\{Y_k^*(\omega)Y_k(\omega)\} \tag{3.13}$$

Where $S_{kk}(\omega)$ is termed as power-spectral density (PSD) of signal $y_k(t)$. Whereas $S_{kl}(\omega)$ denotes cross-spectral density (CSD) between signal $y_k(t)$ and $y_l(t)$. Let $y_k(t) = x_k(t)$ and $y_l(t) = x_l(t)$ using equation (2.11) and equation (3.12), CSD can be expressed as

$$S_{kl}(\omega) = \lim_{T\to\infty} \frac{1}{T} E\left\{ \left(\sum_{r=1}^{n} Z_r(\omega)u_{r,k} \right)^* \left(\sum_{p=1}^{n} Z_p(\omega)u_{p,l} \right) \right\} \tag{3.14}$$

$Z_i(\omega)$ is finite Fourier transformation of $z_i(t)$. Using Fourier theory to equation (2.9) and equation(2.10), $Z_i(\omega)$ becomes

$$Z_i(\omega) = \frac{v_i BQ(\omega)}{j\omega - \lambda_i} \tag{3.15}$$

Substituting equation (3.15) into equation (3.14) results

$$S_{kl}(\omega) = \lim_{T\to\infty} \frac{1}{T} E\left\{ \left(\sum_{r=1}^{n} \frac{vr BQ(\omega)}{j\omega - \lambda_r} u_{r,k} \right)^* \times \left(\sum_{p=1}^{n} \frac{v_p BQ(\omega)}{j\omega - \lambda_p} u_{p,l} \right) \right\} \tag{3.16}$$

For $\lambda_i = \alpha_i + j\omega_i$ with low damping, the value $\alpha_i \ll \omega_i$. Let $\omega = \omega_i$, the approximation of equation (3.16) becomes

$$S_{kl}(\omega_i) \cong \lim_{T\to\infty} \frac{1}{T} E\left\{ (Z_i(\omega_i)u_{i,k})^* (Z_i(\omega_i)u_{i,l}) \right\} \tag{3.17}$$

the term $u_{i,k}$ and $u_{i,l}$ are constant, thus equation (3.18) is obtained

$$S_{kl}(\omega_i) \cong u_{i,k}^* u_{i,l} \left[\lim_{T\to\infty} E\left\{ |Z_i(\omega_i)|^2 \right\} \right] \tag{3.18}$$

Since $\underline{q}$ is random, the $\lim_{T\to\infty} E\left\{ |Z_i(\omega_i)|^2 \right\}$ converges to a real constant value. The value is scaled by the variance of $\underline{q}$. The angle of CSD can be calculated using approximation

$$\angle S_{kl}(\omega_i) \cong \angle u_{i,l} - \angle u_{i,k} \tag{3.19}$$

The PSD can be calculated by setting $k = l$. Thus equation (3.18) becomes

$$S_{kk}(\omega_i) \cong |u_{i,k}|^2 \left[\lim_{T \to \infty} E\left\{ |Z_i(\omega_i)|^2 \right\} \right] \tag{3.20}$$

Base on the derivation above, the mode shape can be estimated using equation (3.19) and equation (3.20). Equation (3.20) indicates that PSD of each signal is scaled by $|u_{i,k}|^2$ thus this can be used to calculate mode shape magnitude. It provides also the observability of modes in state. While (3.19) can be used to calculate the angle of mode shape. The generator k with high observability of mode ω_i is normally selected as reference.

In addition to above spectral analysis functions, the squared-coherency function can be used to measure the coherency of two signals. The squared-coherency function is defined as

$$\gamma_{k,l}^2(\omega) = \frac{|S_{k,l}(\omega)|^2}{S_{k,k}(\omega)S_{l,l}(\omega)} \tag{3.21}$$

If two signals are uncorrelated , the coherency is close to zero. On another hand, if the signals are strongly correlated or coherent, the coherency approaches to one. The coherency function can be used to determined whether the oscillation due to single or multiple mode. If the value of coherency is close to one, the oscillation is caused by single mode.

3.5 Modal Sensitivity Identification

In real-time application, mode sensitivity in equation (2.15) must be approximated from available measurement. Huang, Z., et all. in [18] proposed an idea that mode change from one time instance to another time instance is approximated by linear combination of all power changes in power system i.e generation and load change. Thus, it can be expressed as

$$\Delta\lambda^{(i)} = \frac{\partial\lambda}{\partial P_1}\Delta P_1^{(i)} + \frac{\partial\lambda}{\partial P_2}\Delta P_2^{(i)} + \cdots + \frac{\partial\lambda}{\partial P_N}\Delta P_N^{(i)} + \varepsilon^{(i)} \tag{3.22}$$

$\Delta\lambda$ is mode change from previous time at time instance i. $\Delta P_N^{(i)}$ denotes the power changes at time instance i. $\frac{\partial\lambda}{\partial P_N}$ is mode sensitivity with respect to power change at P_N And ε represents noise measurement. After M time instant, the equation (3.22) can be expanded into matrix form

$$\begin{bmatrix} \Delta\lambda^{(1)} \\ \Delta\lambda^{(2)} \\ \vdots \\ \Delta\lambda^{(M)} \end{bmatrix} = \begin{bmatrix} \Delta P_1^{(1)} & \Delta P_2^{(1)} & \cdots & \Delta P_N^{(1)} \\ \Delta P_1^{(2)} & \Delta P_2^{(2)} & \cdots & \Delta P_N^{(2)} \\ \vdots & \vdots & \ddots & \vdots \\ \Delta P_1^{(M)} & \Delta P_2^{(M)} & \cdots & \Delta P_N^{(M)} \end{bmatrix} \begin{bmatrix} \frac{\partial\lambda}{\partial P_1} \\ \frac{\partial\lambda}{\partial P_2} \\ \vdots \\ \frac{\partial\lambda}{\partial P_N} \end{bmatrix} + \begin{bmatrix} \varepsilon^{(1)} \\ \varepsilon^{(2)} \\ \vdots \\ \varepsilon^{(M)} \end{bmatrix} \tag{3.23}$$

The power change ΔP must follow the power balance equation i.e.

$$\sum P_i = \Delta P_1^{(i)} + \Delta P_2^{(i)} + \cdots + \Delta P_N^{(i)} = 0 \tag{3.24}$$

This equation shows that the set of equation is linearly dependent, and it causes ill-conditioned problem. If one solves equation (3.23) the result can be misleading. The solution can be achieved by leaving out one power measurement e.g. P_1 and one can obtain a set of linearly independent equation. Thus equation (3.23) changes to

$$
\begin{bmatrix} \Delta\lambda^{(1)} \\ \Delta\lambda^{(2)} \\ \vdots \\ \Delta\lambda^{(M)} \end{bmatrix} = \begin{bmatrix} \Delta P_1^{(1)} & \Delta P_2^{(1)} & \cdots & \Delta P_N^{(1)} \\ \Delta P_1^{(2)} & \Delta P_2^{(2)} & \cdots & \Delta P_N^{(2)} \\ \vdots & \vdots & \ddots & \vdots \\ \Delta P_1^{(M)} & \Delta P_2^{(M)} & \cdots & \Delta P_N^{(M)} \end{bmatrix} \begin{bmatrix} \frac{\partial\lambda}{\partial P_2} - \frac{\partial\lambda}{\partial P_1} \\ \frac{\partial\lambda}{\partial P_3} - \frac{\partial\lambda}{\partial P_1} \\ \vdots \\ \frac{\partial\lambda}{\partial P_N} - \frac{\partial\lambda}{\partial P_1} \end{bmatrix} + \begin{bmatrix} \varepsilon^{(1)} \\ \varepsilon^{(2)} \\ \vdots \\ \varepsilon^{(M)} \end{bmatrix} \tag{3.25}
$$

in order to distinguish generation and load measurement, the load measurement is denoted as negative of generation.

The mode sensitivity result in equation (3.25) is termed as relative mode sensitivity which is in this case it is relative to P_1. Relative mode sensitivity is more meaningful for example $\frac{\partial\lambda}{\partial P_2} - \frac{\partial\lambda}{\partial P_1}$ denotes the sensitivity of the mode when P_2 is increased and P_1 is decreased. This technique requires pair action i.e. one generation is increased and one is decreased. One can easily transform from relative sensitivity with respect to particular generation to another reference.

In real-time application, ΔP can be obtained from power measurement such as PMU or SCADA measurement while $\Delta\lambda$ can be calculated from system identification techniques. This approach can give the recommendation action for power system operator to improve the stability condition.

CHAPTER IV

PHASOR MEASUREMENT UNIT

4.1 Definition

Reference [28] defines a PMU as device capable of long term recording of electrical characteristics and disturbances in phasor format and providing continuous phasor measurements. Normally PMU measures phasor voltage and phasor current as well as the bus frequency. Phasor voltage measurement is referred to bus voltage in which PMU is installed. Current measurement of PMU is the current flowing from/to the PMU bus. While the frequency also refers the bus frequency of PMU bus.

The application of PMU in power system is described in the Figure 4.1 [29]. PMU is usually placed into several buses in power system. The measurement data is then sent to data concentrators before being used for various applications such as protection, monitoring, control, etc.

4.2 Development

The History of PMU has experienced a long development [10]. There have been a significance interest from many power engineers to measure phase angle of voltage for many years. It is motivated by the strong relationship between voltage angle difference and real power flow. Since real power flow is one of main interest in power system study, the effort to improve the technique keep progressing.

The earliest modern effort was reported in [30], [31], [32]. It utilized LORAN-C, GOES satellite transmissions, and the HBG radio transmissions (in Europe) to achieve synchronized measurement. The technology used the zero crossing to calculate the phase angel of voltage with respect to the references. After calculating voltage angle difference with respect to the reference, the phase angle difference between two buses in power system can be calculated. Using this technology, the accuracy of 40 μs could be achieved. However, the technology had several drawbacks. First, the presence of harmonic waves was ignored thus it affected the accuracy. Moreover, the phasor magnitude measurement was also neglected. The absence of these importance keys made this method was not suitable for generalized wide area phasor measurement system.

The next stage of PMU was hugely boosted by the effort made to calculate symmetrical component in power system. Reference [33] published a novel technique to calculate the symmetrical component with fast and accurate algorithm. The theory described the technique for computing symmetrical component of three phase voltage and current. Soon, it was revealed that positive sequence as a part of symmetrical component had important information for power system analyze [34]. This stage was the kick-started of modern phasor measurement development.
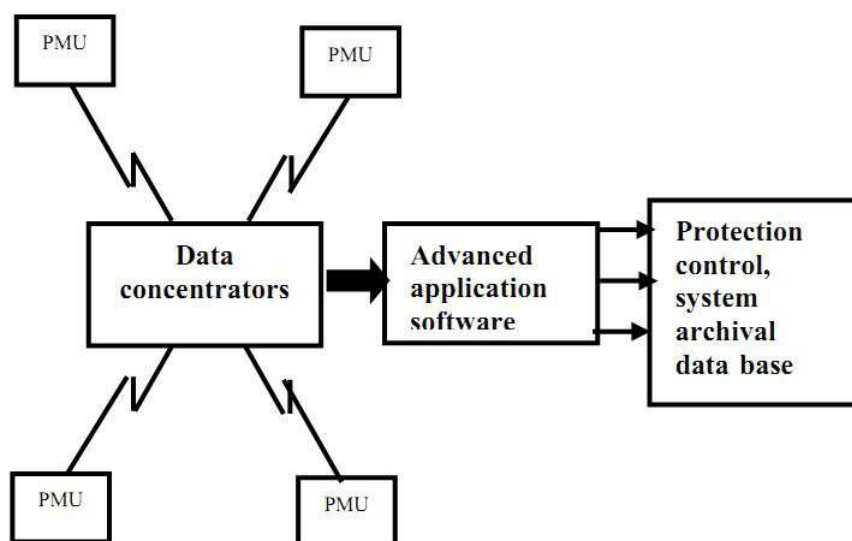
Figure 4.1: PMU in power system
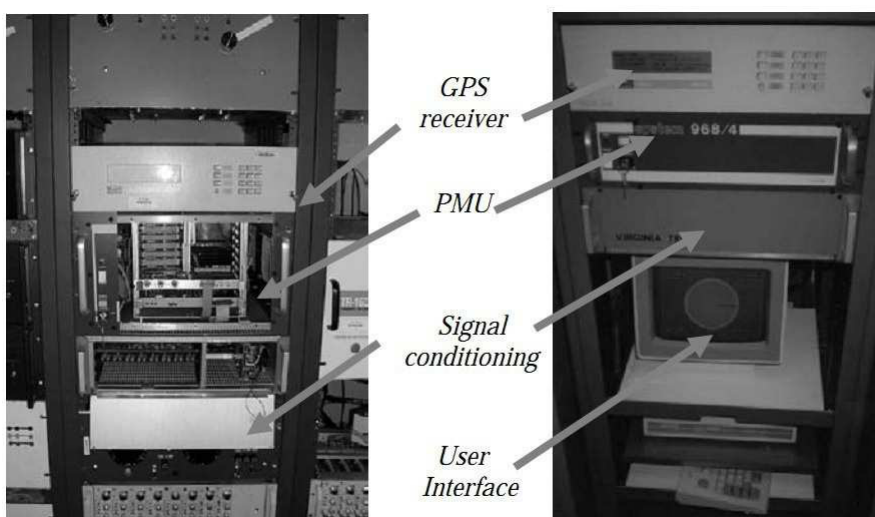
Figure 4.2: First GPS-based PMU built by Virginia Tech

Around 1980s, the Global Positioning System (GPS) has entered mature technology and it was obvious that GPS could be deployed as synchronizing reference of power system measurement. The first GPS-based PMU was made at Virginia Tech in the early 1980s. The prototype can be seen in Figure 4.2. The prototype then installed at several buses at Bonneville Power Administration, the American Electric Power Service Corporation, and the New York Power Authority. The commercial production of PMU did not take a long time to wait as in 1991 Virginia Tech collaborated with Macrodyne. Now, some companies offer mass production of PMU. In order to standardize the PMU, in 1991 IEEE issued a standard for PMU [35] and it was revised in 2005.

4.3   Requirement

According to [28], in order to work properly, a PMU and supporting component should have following capabilities:

4.3.1   Functional

1. Should have at least 15 analog inputs and 8 digital (event) inputs.

2. Should have Uninterruptible Power Supply (UPS) capable of operating the recorder for at least eight hours in case of loss of main power.

3. The data interface should be compatible with PC.

4. PMU Should have one or more data ports

5. A frequency response of 0-10 Hz minimum.

6. A sample rate between 20 samples per second and 60 samples per second with flexibility of the user to select.

7. Data resolution no less than 12 bit

4.3.2   Time Tagging Capability

1. Capable of interfacing with satellite time clock.

2. Phase angle accuracy within 1 degree.

3. Events to be time tagged to within $\pm$ 50 μs.

4. Backup clock shall be provided to time events in case of GPS failure.

4.3.3   Measurable Data

The minimum output of PMU measurement should include at least:

1. Positive sequence voltage and current .

2. System frequency - based on monitoring selected channel(s) of input voltage(s).

3. Phase Angle - the monitor must produce a voltage and current phase angle. When used with other system monitors, the voltage phase angle between buses can be measured.
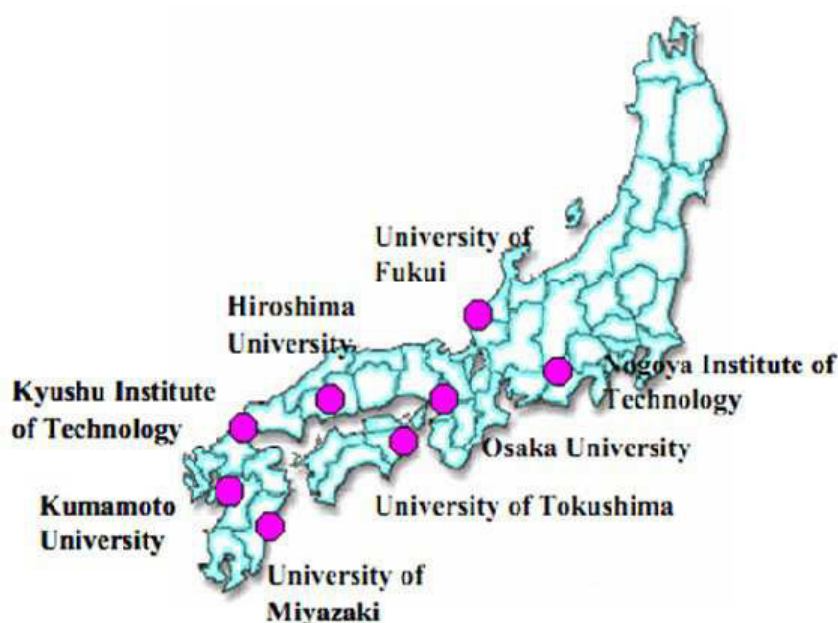
Figure 4.3: PMU location in Western Japan 60-Hz System

4.4 Application for Inter-area Power Oscillation

Due to many advantages of PMU, it has been widely used for many purposes related to inter-area power oscillation identification and monitoring. There are a lot of previous work that have been done to utilize PMU for inter-area power oscillation. One of the example is campus WAMS application. It is developed by researcher at Kyushu Institute of Technology, Japan [36]. They developed the campus WAMS due to the difficulty to get data access from the power system utility. The FFT is used to estimate the mode from the measurement. The PMU is installed at eight universities at Japan using PMU from Toshiba NCT2000 Type-A. In addition, The application is also installed at three universities in Thailand. The PMU locations in Japan and Thailand can be seen in the Figure 4.3 and Figure 4.4 respectively.

The PMUs measure the single phase voltage of 100 V (in Japan) and 220 V (in Thailand) from the outlet on the wall of laboratory with GPS-synchronized time tag. A sinus wave is sampled using 96 sample data. The time windows of the data are 50 minutes to 10 minutes and 20 minutes to 40 minutes using interval $1/30$ s. From the measurement two inputs can be extracted i.e. phase difference between two locations and frequency deviation of one location. The FFT is used to provide initial understanding of the inter-area oscillation. The complete process is illustrated in the Figure 4.5.

Meanwhile, the Pacific Northwest National Laboratory (PNNL) in USA has also been carrying out the research about the monitoring of grid stability using synchronous measurement. This is because North America power grid has experienced many black out including system collapse on Aug 10th, 1996. The research is a collaborative research between PNNL, the University of Wyoming, Montana Tech of the University of Montana, Bonneville Power Administration and Electric Power

Figure 4.4: PMU locations in Thailand system
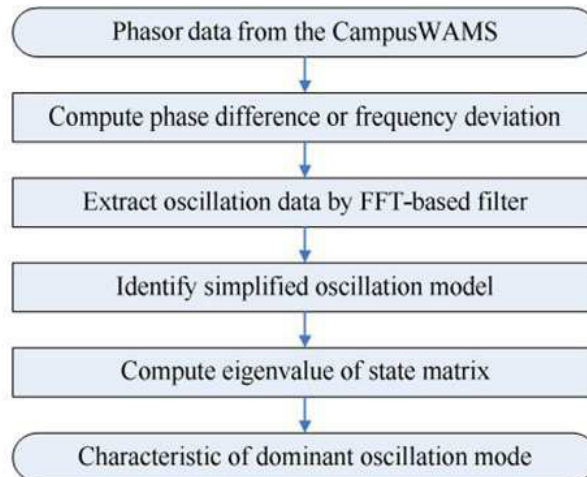
Figure 4.5: Complete estimations process

Group.

One of the appearance of monitoring system is illustrated in the Figure 2 8. The figure shows the data record during system collapse on Aug 10th, 1996. The output is shown in the GUI which include the PSD of the signal and the location of estimated modes in the *s*-plane with its respective damping and frequency. The regularized robust recursive least squares (R3LS) algorithm is deployed in this application [37]. The demo playback of this monitoring system can be found in the PNNL website [38].
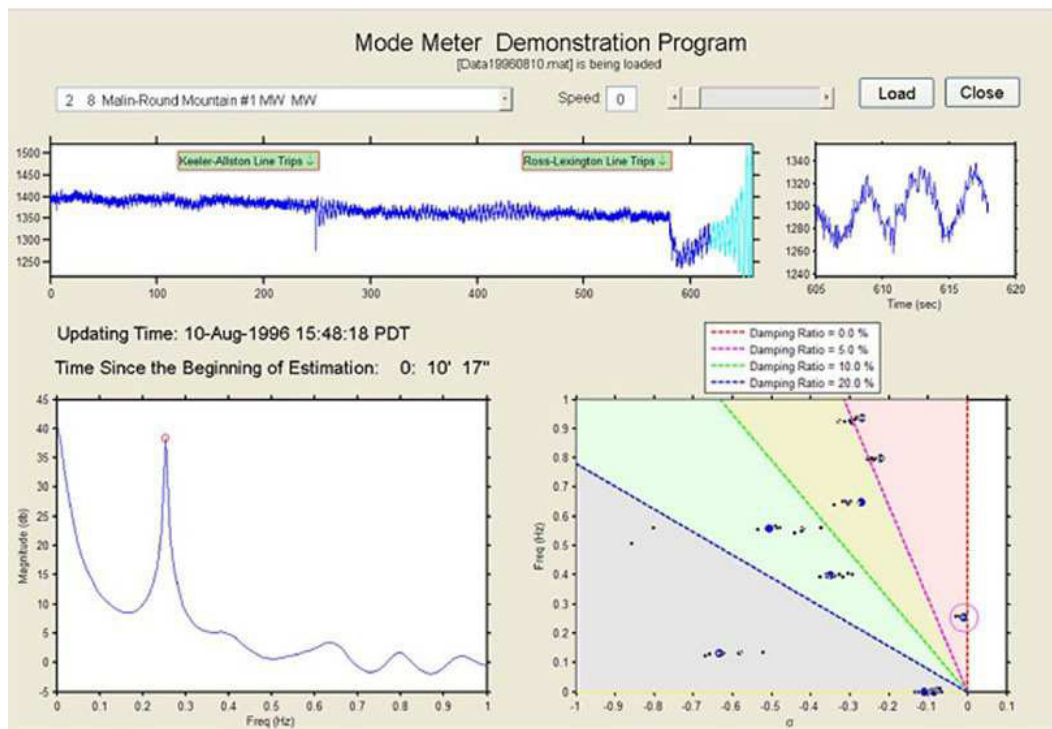
Figure 4.6: Mode-meter demonstration program

CHAPTER V

REAL-TIME POWER OSCILLATION MONITORING SYSTEM

This chapter presents the development of real-time power oscillation monitoring system. Section 5.1 starts by explaining the concept PMU placement. The order selection of system identification is discussed in Section 5.2. Section 5.3 presents the application development of real-time power monitoring system including preprocessing data, modal properties identification, and modal sensitivity identification. The last section, Section 5.4, gives the GUI appearance to display the important information related to stability condition. Figure 5.1 shows the several steps in developing the real-time monitoring system.

5.1   PMU Placement

PMU location is very essential for inter-area modes identification since it affects the accuracy of the outcomes. Therefore, careful study should be performed to determine the PMU location in power system. PMU placement is strongly influenced by the type of analysis that want to be carried out. In general, there are two analysis used in this research. First, the MYW method is used for mode frequency and mode damping identification. Second, Spectral analysis, consisting of PSD and CSD function, is deployed to identify the mode shape. The PMU location selection for these analysis should be considered independently. The overall PMU location selection process is given in the Figure 5.2.

The selection of PMU location for mode frequency and mode damping estimation utilizes the observability concept based on PSD function in equation (3.20). PSD function measures the observability of inter-area modes in the measurement signal. The inter-area modes will show up as a significance peak at particular frequency in PSD graph. Signals with good modes observability, i.e. whose have significance peak, are selected to locate PMU. Here, voltage angle difference is used as the input signal. The process is depicted in the lower part of Figure 5.2. Reference [39] demonstrates how to use the concept.

Meanwhile, in order to select proper location of PMU for mode shape estimation, the coherency analysis in equation (3.21) is utilized. Using coherency analysis, the group of coherence generator can be identified. The frequency of generator bus is used as the input for square coherency function. One group of coherent generator can be represented by single PMU measurement. In one coherence group, the generator normally will exhibit coherently. Thus, there is no need to measure every generator in the group. The Upper part of Figure 5.2 shows the process of locating PMU for mode shape identification.
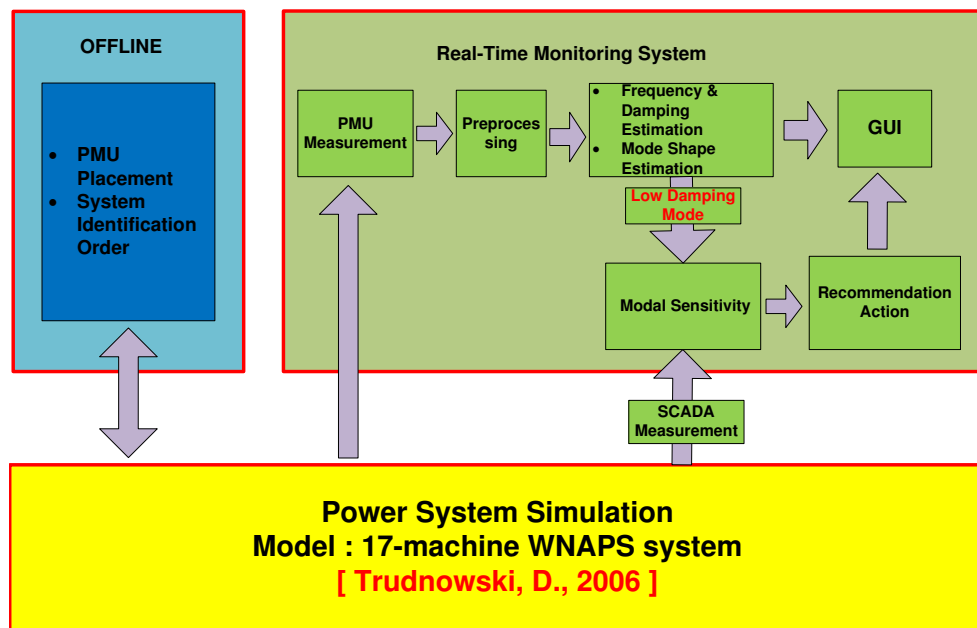
Figure 5.1: Development of real-time power oscillation monitoring system
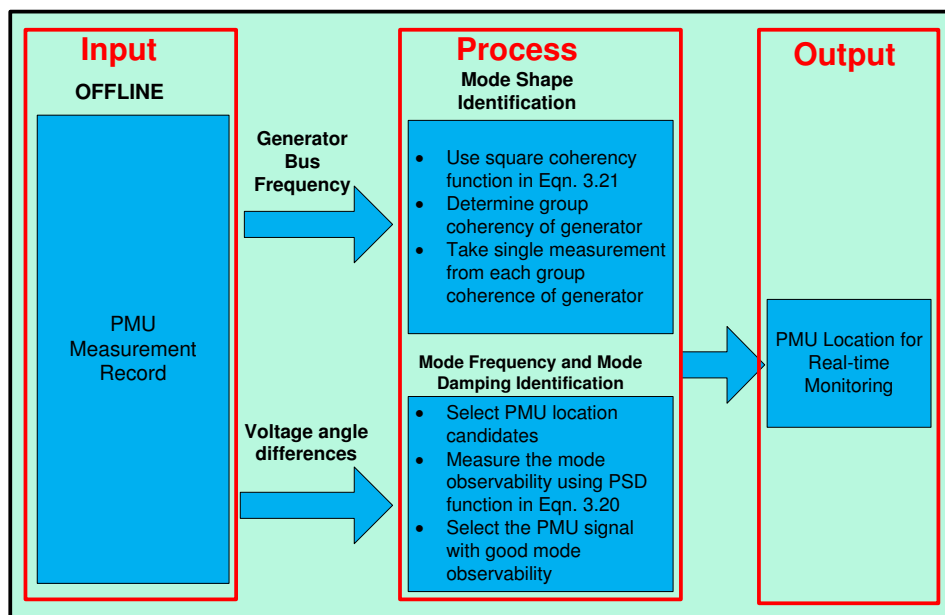
Figure 5.2: PMU location selection

Based on the experience of the author, the group of coherent generator is usually formed by several generators connected at the same bus. In this condition, single frequency measurement from generator bus is enough to represent the rest of generators. This rule of thumb is illustrated by Figure 5.3, and it can be seen that bus 2 and bus 4 comprise of two generators at each bus. However, the measurement requires only one PMU from each bus and there is no need to install 2 PMU at bus 2 or bus 4.
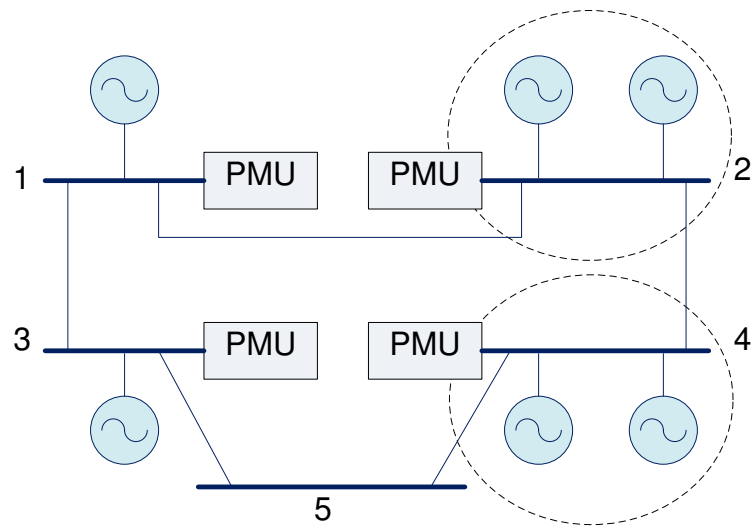
Figure 5.3: Example of PMU location

5.2 Order Selection

Section 3.3 has intensively elaborated the Modified Yule-Walker (MYW) algorithm to identify mode frequency and mode damping of inter-area power oscillation. As it can be seen, the mode frequency and mode damping result depends on three parameters of MYW i.e. M, N, and P. They denote the order of nominator, denominator, and the number equation used, respectively.

The true order of the system is often unknown. Therefore, the high order of M, N, and P are normally preferred [19]. Reference [19] also suggests to use high number of N to improve numerical condition with typical value N is 20 to 25. The result can be readily compared with the result from modal analysis to analyze the accuracy.

5.3 Application Development

The Application development is presented in this section. It covers the green box in the Figure 5.1. Once system order selection and the proper location of PMU for estimating mode frequency, mode damping and mode shape has been selected, they can be used for real-time monitoring identification. The location and the identification parameters need not to be changed as long as the system structure does not change either. In contrast, The offline procedure should be revisited if the system structure changes.

Real-time monitoring system uses real-time data flow from PMU, and the identification process is continuously performed. However, the data should be preprocessed before being used. After preprocessing, the data then can be used to identify the mode frequency, mode damping and mode shape of inter-area oscillation. If the mode with low damping is detected, the operator may activate modal sensitivity application to obtain recommendation action for improving the mode damping.
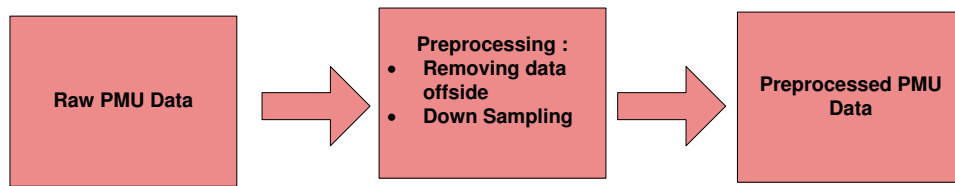
Figure 5.4: Data preprocessing

Modal sensitivity requires the generation and load measurement which can be readily obtained from SCADA measurement. This is the reason why the real-time application should be compatible with other monitoring systems e.g. SCADA system.

The final step is to display all identification results i.e mode damping, mode frequency, mode shape, and recommendation action in Graphical User Interface (GUI). GUI can assist the operator to monitor the system stability real-time. The absence of GUI can make the operator have problem in interpreting the results. In addition, GUI should be easily understood and interactive.

The subsequent section explain the detailed processes of the application development for real-time monitoring.

5.3.1 Preprocessing Data

The data from the PMU measurement should not be used directly for identification process since it may contain some offset or noise. In addition, the data may also have very high sampling rate. These factors can deteriorate the results of mode identification. Therefore, it is necessary to preprocess the data before being used. The preprocessing stage is given in the Figure 5.4 and it includes removing data trend and down sampling. The first step, i.e. removing the offset, is necessary due to the assumption that system is perturbed around its stationary point. Matlab has built-in function *detrend* to remove data offset. On the other hand, down sampling data is also necessary since the data measured by PMU usually has very fast sampling rate. Inter-area oscillation is always a slow phenomenon thus the sampling rate does not need to be very fast. Here, the PMU is set to have sampling rate 30 samples/sec. The data is then down sampled to 5 samples/sec. This sampling rate still obeys the Nyquist sampling theorem.

5.3.2 Modal Properties Identification

After preprocessing, the data is ready for identification process. The process includes the mode frequency and damping estimation and mode shape estimation. The Modified Yule-Walker method is performed to estimate both the frequency and damping of inter-area oscillation modes. Voltage angle difference is used as the input for this algorithm. The detail of the modified Yule-Walker method has been explained previously in the section 3.3. The subsequent process is to use the mode selection algorithm to identify the dominant modes of inter-area oscillation. Mode selection is necessary to
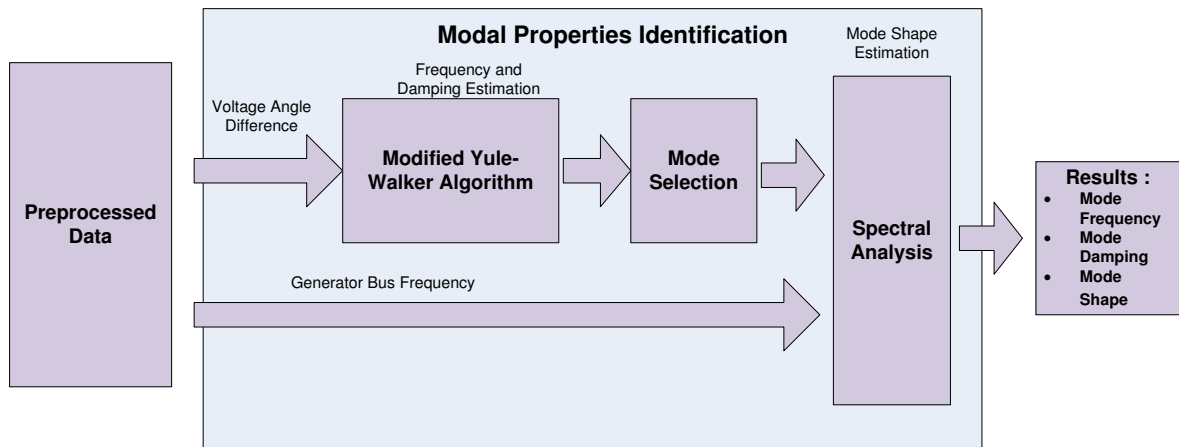
Figure 5.5: Modal properties identification process

select the mode having high energy in the input signal.

In the other hand, to identify mode shape of the inter-area oscillation, the spectral analysis is used. It requires generator bus frequency as the input. Spectral analysis consists of two functions, i.e. Power Spectral Density (PSD)and Cross Spectral Density (CSD), as having been explained in the section 3.4. The bus with the highest PSD value is set to be the reference bus for calculating mode shape magnitude and angle. The mode frequency estimation from Modified Yule-Walker is then also used as the input to spectral analysis in order to estimate the corresponding mode shape. The overall process of the modal properties identification is given in the Figure 5.5.
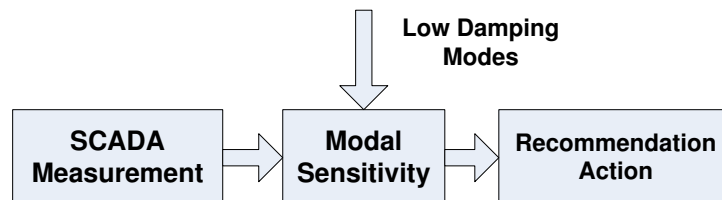
Figure 5.6: Recommendation action

5.3.3   Modal Sensitivity Identification

Modal sensitivity is estimated in real-time monitoring using Equation 3.25. The right side of the equation comprises of generation and load power. This measurement normally can be obtained directly from SCADA measurement. The left side of the equation is given by the result of modal identification. However, the modal identification used in this research, i.e. MYW algorithm, has major shortcoming since it often requires quite long time windows to obtain accurate result. As consequence, the left side of the equation is ill-conditioned, and moreover, it does not represent the current system condition. In long time window, more recent data should be weighted more than older data to yield good result. To overcome the problem, this research uses non-linear mapping of
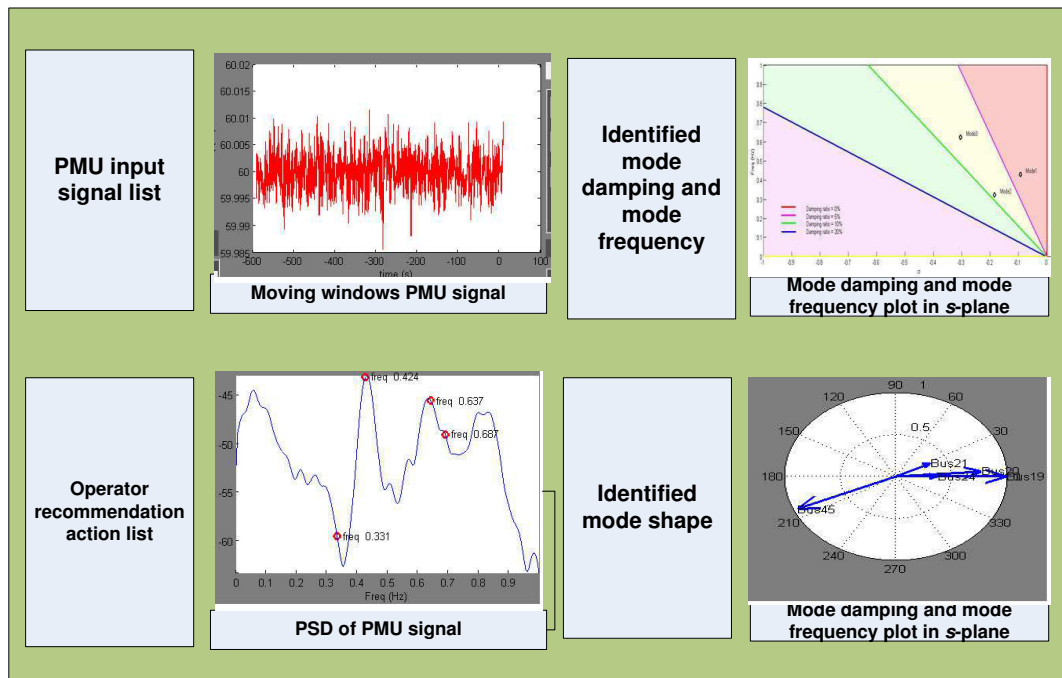
Figure 5.7: GUI concept

generation and load power changing to eigenvalues changing. It uses nonlinear function based on Artificial Neural Network (ANN). ANN-based function allows using short data in order to produce more accurate left side of Equation 3.25. The training data for ANN can be obtained using historical data in control center. The mapping function is only used when the modal sensitivity identification is performed.

It is unnecessary to run modal sensitivity all the time. The operator can choose running this application only when mode with low damping is detected. The output of modal sensitivity analysis is recommendation action which can serve as a guidelines for the operator to improve mode damping. The recommendation can be several actions consisting of both increasing and reducing output of generator pair at the same amount. The detail of the process is presented in the Figure 5.6.

5.4 GUI Development

The GUI is designed to help the operator in monitoring power system stability real-time. It should, at least, display the information from identification results i.e. mode frequency, mode damping, mode shape and operator recommendation. It may also provide other features for the sake of convenient to the operator. GUI should be interactive as such operator can easily select what want to be displayed in the screen.

In this research, the concept GUI display is shown in the Figure 5.7. It can be noticed that basically the GUI is divided into four column. The most left column contains the name of PMU signals used as the input and the list of recommendation action for the operator. One can select the PMU
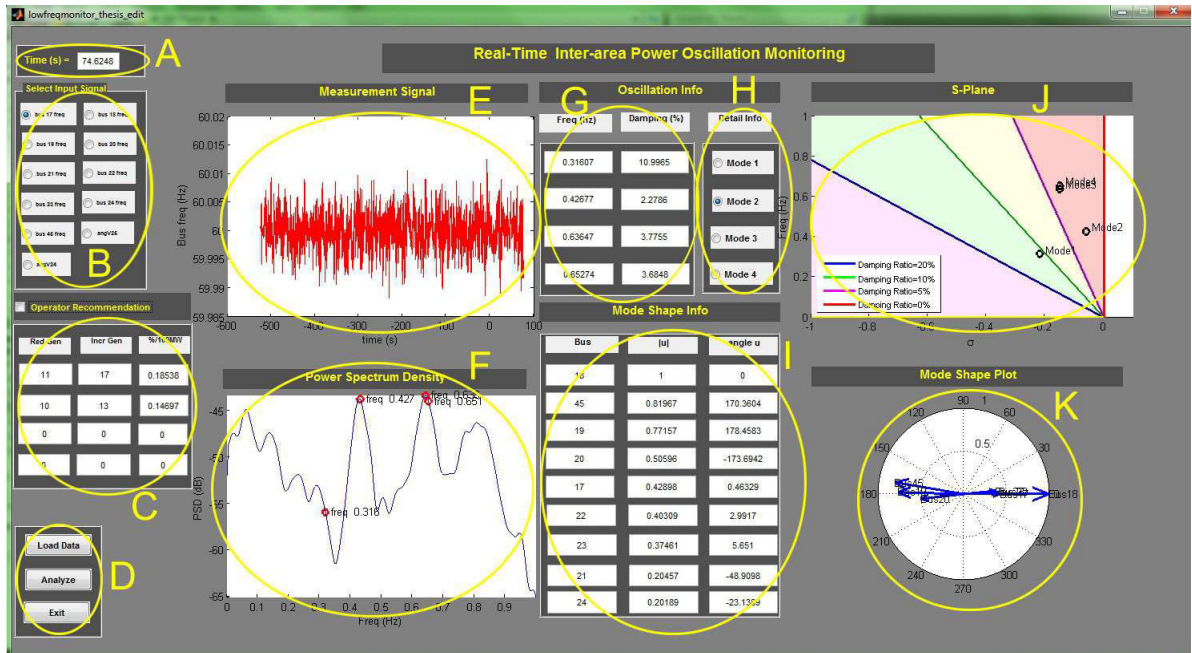
Figure 5.8: GUI appearance

signal's name to display corresponding signal on moving window plot. The PSD of the corresponding signal is also automatically presented on PSD plot. The mode damping, mode frequency, and mode shape are presented numerically in the form of table in the third column. The fourth column displays mode damping, mode frequency, and mode shape graphically. Mode damping and mode frequency are displayed in the s-plane. The s-plane has been divided into several regions representing the damping range based on the division in [37]. While, the mode shape plot displays the compass plot indicating the interaction among generators in the particular mode oscillation. The plot can be easily changed by choosing corresponding mode's name. All the information in the GUI appearance is updated real-time.

The GUI is developed based on the concept presented in the passage above. The basic requirement is that it should display the information resulted from identification analysis to assist the operator in monitoring process. The display can also include other information such as the time and various signals graph. Other features are that GUI should be user friendly and interactive, therefore the operator can display what is required.

Matlab GUI [40] provides extensive features to build graphical user interface. The GUI presented in this research is based on Matlab GUI. Figure 5.8 shows the final appearance of GUI for real-time monitoring of inter-area power oscillation. One can take a look that the GUI has 11 main features encircled by yellow circle with its corresponding alphabet. The section A of the GUI informs the current time step in the simulation, and it is updated every 0.2 second. Section B lists all the PMU's signal names i.e. generator bus frequency and voltages angle difference. The operator can select any PMU signal that want to be displayed in section E by clicking the signal name in the section

B. The corresponding PSD of PMU signal is also presented in section F and it changes automatically whenever the operator changes the signal name in section B.

Section C presents the list of recommendations to improve the damping of inter-area modes. It contains maximum four pair actions, i.e. increasing and decreasing generator pairs. The operator can select a list of recommendations for particular mode by selecting mode's name in the section H. The program can possibly provide recommendation actions less than 4 if it can only find less than 4 possible actions. To start and stop the program as well as load initial artificial data, the push buttons in section D can be selected accordingly. Initial artificial data is necessary for starting up the simulation, and later it is removed automatically when the time window is long enough.

The result of MYW algorithm and spectral analysis are presented in the section G and I. Section G consists of mode frequency and mode damping of the system and then they are plotted in the s-plane, i.e in section J, to make the monitoring easier. The s-plane is divided into several regions representing the damping ranges. The division representation follows the work in [37]. In addition, the result of mode shape identification is presented in the section I and section K in the form of table and graphical, receptively. The operator can change the mode shape of particular mode by clicking the mode name in section H.

CHAPTER VI

PERFORMANCE VERIFICATION

The test system and test conditions for evaluating the real-time monitoring system are presented in this chapter. Section 6.1 introduces the test system used to perform the simulation. It consist of the representation of power system, PMU, and real-time system. The results of PMU placement and system order selection for corresponding power system are given in Section 6.3 and Section 6.2, respectively. While, Section 6.4 designs the conditions for assessing the accuracy and reliability of real-time monitoring system. The simulation is performed using computer with specification: processor = Intel core i7-3520 M @2.9 GHz, memory = 8192 MB RAM.

6.1 Test System

6.1.1 Power System Representation

In this research, power system measurement is taken from the simulated power system using Power System Toolbox (PST) [41]. PST is developed based on the Matlab *m*-files environment. It allows the user to analyze the power system in time domain simulation as well as the modal analysis. In addition, PST provides complete library of generator type, load type, power system network, event, control apparatus and so on.

The simplified 17 machine Western North American Power System (WNAPS) [11] is used to evaluate the performance of proposed method. The system is shown in the Figure 6.1. All generators are modeled as detailed two-axis transient model. Generator 1–8 and 17 are without governor. Generator 9–16 are equipped with speed governor with the detail generator 9, 10, 14 and 16 use hydro turbine and generator 11, 12, 13 and 15 use steam turbine. In addition, PSSs are used in all generation units. From the Figure 6.1, it can be observed that the system consists of major generation buses 17 through 24 and bus 45. The complete system parameters are given in Appendix.

The load is modeled as a portion of constant current, constant power, constant impedance and random load. The random load is characterized as random low-pass filtered Gaussian White Noise ($1/f$ filter), and it is used to resemble small random load variation in real power system.

The 17 machine system can be linearized using PST with total system order is 203rd. This analysis is popular as modal analysis. The result is shown in the Table 6.1. It can be recognized that the system consists of four inter-area modes with the frequency 0.3179, 0.4219, 0.6349, and 0.6730 Hz. The 0.4219 Hz mode has the lowest damping among any other modes with damping value is 3.6275 %. This mode is an interaction between northern half system swings against southern half and bus 45. The mode shape of mode 0.4219 Hz confirms this interaction. The mode shape of 0.4219 Hz
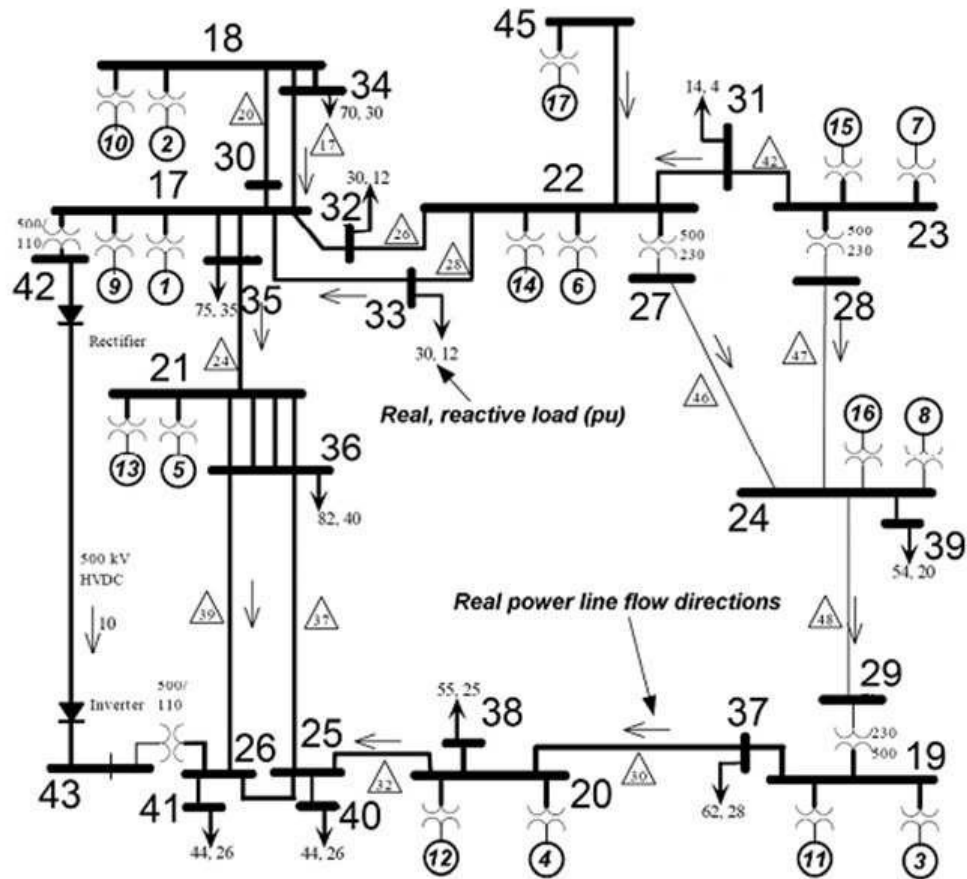
Figure 6.1: WNAPS 17 machine system

mode is shown in the Table 6.2. Bus 18, 45, 19, 17 and 22 are strongly participated in this oscillation with bus 18, bus 17 and bus 22 swing against bus 45 and bus 19. To obtain these properties, modal analysis requires around 2.289441 seconds for single operating condition. Thus, it is not possible for real-time monitoring purpose.

Table 6.1: Inter-area modes of 17-machine system

Frequency (Hz)	Damping (%)	Bus vs Bus
0.3179	10.7394	Northern half vs Southern half
0.4219	3.6275	Northern half vs Southern half+bus 45
0.6349	3.9370	Bus 18 vs. Rest of system
0.6730	7.6347	Bus 20,21 vs. bus 24

To improve the damping of 0.4219 Hz, one can calculate the modal sensitivity using perturbation theory in Equation 2.15. The base case is set to the condition whose mode frequency is 0.4219 Hz and mode damping is 3.6275 %. From the base condition, generation and load is changed randomly to generate 1000 cases. For each case, the corresponding mode frequency and mode damping are calculated using modal analysis. The result is given in the Figure 6.2. It can be analyzed that

Table 6.2: Mode shape of 0.4219 Hz mode

Bus	$|u|$ (normalized)	$\angle u$
18	1.00	0
45	0.8569	-183.1249
19	0.5959	-168.6048
17	0.4305	-0.8470
22	0.4007	-2.5455
23	0.3786	-7.2351
20	0.3727	-167.8277
24	0.1507	-21.9713
21	0.1404	13.5787
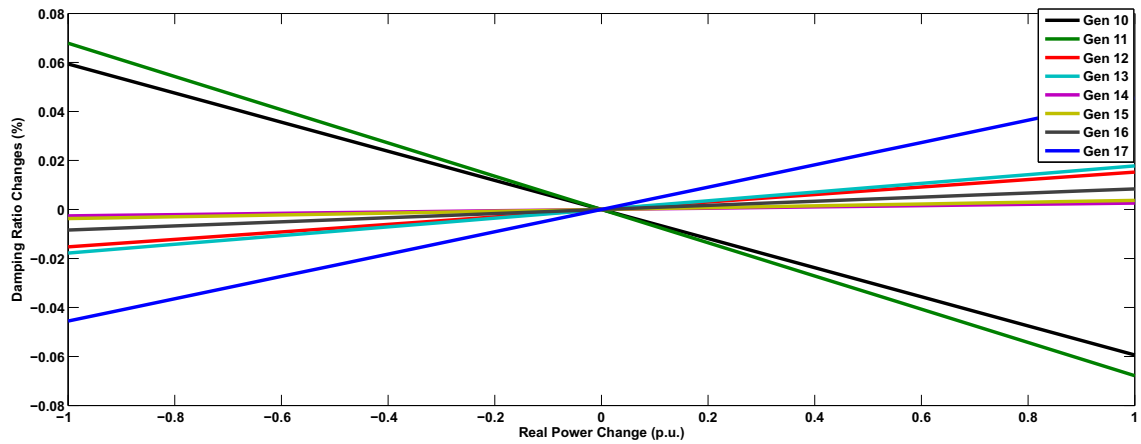
Figure 6.2: Modal sensitivity of mode 0.4219 Hz

generator 11 and 17 form the most effective pair to improve the damping of 0.4219 Hz mode. It can be carried out by increasing the output of generator 17, and at the same time reducing the output of generator 11 with the same amount. By doing this pair action, the operating condition is redistributed and the power system moves to more stable operating condition. Another possible pair is generator 10 and generator 13, although they are less effective than the first pair. Increasing the output of generator 13 and reducing the output of generator 10 will also have capability to improve the damping of mode 0.4219 Hz.

The modal sensitivity is very important to the power system operator since it gives the recommendation action to improve the damping. Without this analysis, operator can possibly choose inappropriate action that will degrade the system condition such as choosing to reduce output of generator 17 and increase the output of generator 11 instead. This analysis also allows the operator to pick up the most effective action.
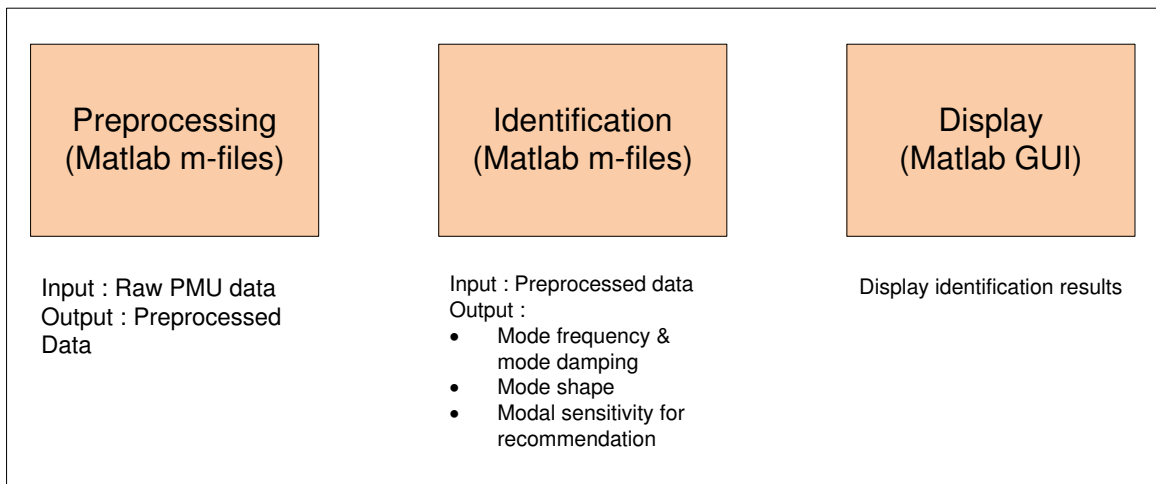
Figure 6.3: Real-time system representation

6.1.2 PMU Representation

Having studied the characteristic of PMU in Section 2, the PMU in this thesis is represented by following aspects:

1. The ability of PMU to measure the phasor quantity of voltage on the bus in which PMU is installed [9].

2. The ability of PMU to measure the bus frequency [8].

3. The sampling rate is set to be 30 samples/sec. This sampling is considered to resemble PMUs sampling rate [7].

6.1.3 Real-Time System Representation

The detail of the real-time system has been presented in Section 5.3. In general, the real-time system comprises three parts i.e. preprocessing, identification, and display. For real-time simulation, preprocessing and identification are set up in Matlab *m*-files. While, the display is built in Matlab GUI environment. Figure 5.3 shows the representation of real-time system. The *m*-files and GUI should be coordinated together with power system simulation in PST to achieve real-time monitoring.

6.2 PMU Placement

This section discuss about the concept of choosing proper location of PMU for the system in Figure 6.1. The process depends on the type of analysis. Section 6.2.1 demonstrates the PMU placement for mode frequency and mode damping Identification. While, PMU placement for mode shape identification is given in the section 6.2.2.

6.2.1 PMU Placement for Mode Frequency and Mode Damping Identification

The idea of PMU placement in this section is in line with what have presented in reference [39] i.e. by extending the concept of mode observability using PSD function approach. There are four important steps offered by [39] i.e. choosing the location candidates, calculating the PSD, selecting the mode having good observability, and finally validating the result with MYW algorithm.

In this research, during offline analysis, four candidates for PMU placement, i.e. bus 25 vs 21, 45 vs 20, 22 vs 17, 24 vs 21, are selected. Note that other candidates can also be selected. The voltage angel difference is then measured. The term bus 25 vs 21 denotes the voltage angle difference between bus 25 and bus 21 in radian unit. Standard measurement of PMU allows direct measurement of voltage angle difference, thus it has practical reason. Voltage angle has also strong relationship with power oscillation. The PSD graph of these four signals is given in the Figure 6.4.

From the Figure 6.4, it can be observed that the PSD graph has a significant peak at particular frequency. The peaks are due to the activity of inter-area modes, and they coincide with inter-area modes in Table 6.1. Single PSD graph normally has only one or several peaks, which means it has only one or several modes, not all modes. For example PSD graph of 25 vs 21, i.e voltage angel difference between bus 25 and bus 21, has significance peak at frequency around 0.3, 0.4, and 0.6 Hz. While, PSD of bus 45 vs 20 has significance peak at frequency around 0.3 and 0.6 Hz.

By looking at the PSD graph, one can intuitively select the signal which will be used for inter-area modes identification. It depends on the mode that want to be extracted. For example PSD graph of bus 25 vs 21 is expected to have good observability of the first three modes, i.e. 0.3179 Hz, 0.4219 Hz, and 0.6349 Hz since it has significance peak around those frequencies. It also implies that signal bus 25 vs 21 may not serve a good result for 0.6730 Hz mode extraction. The PSD of signal bus 25 vs 21 has similar shape to that of bus 22 vs 17. Thus, it may be an alternative for estimating the first three modes. In addition, signal bus 45 vs 20 has significance peak at the frequency around 0.3 and 0.6 Hz. The last signal , i.e bus 24 vs 21, has significant peak only at frequency 0.6 Hz.

Finally, one can pass the four input signals to MYW algorithm to extract the modes. The result is presented in the Table 6.3. They are consistent with the PSD graph. However, in this research to identify the first three modes , i.e. 0.3179 Hz, 0.4219 Hz, and 0.6349 Hz, the bus 25 vs 21 is preferred. It has slightly more accurate results than that of bus 22 vs 17. Meanwhile, the bus 24 vs 21 is used for tracking the remaining mode i.e. 0.6730 Hz mode as the PSD graph also suggested that it has good observability around that frequency.

In summary, the mode frequency and mode damping require at least 3 PMUs installed at bus 25, bus 24, and bus 21. Other selections are possible, but it must consider the mode observability and minimum PMU number installation.
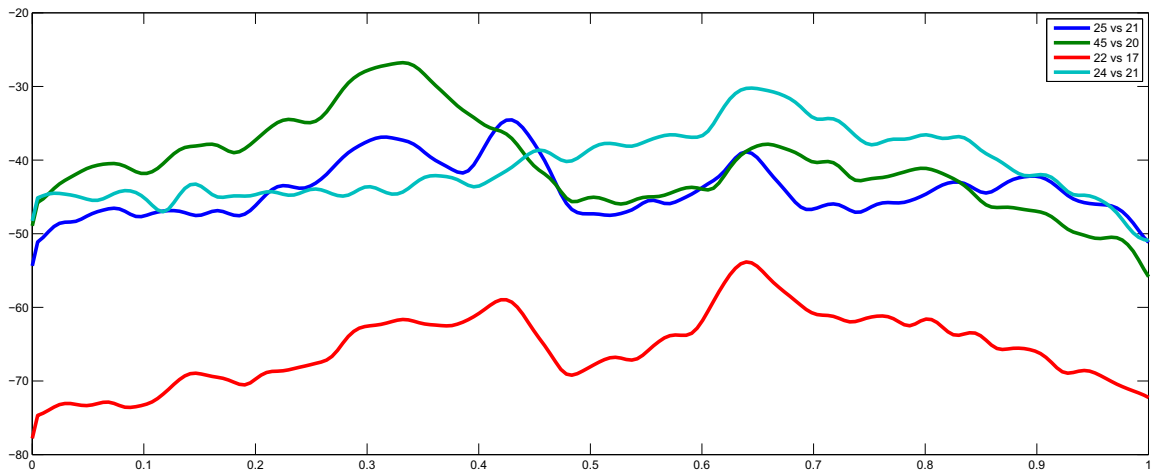
Figure 6.4: PSD graph for PMU placement

6.2.2 PMU Placement for Mode Shape Identification

This section demonstrates the PMU location selection for mode shape identification. The square coherency function in Equation 3.21 is used to select group of coherence generator. The single measurement is taken from each coherence group. Matlab has built-in function to calculate square coherency function by using function *mscohere*. The function *mscohere* returns the square coherency magnitude at each frequency. The magnitude ranges between 0 and 1, and it measures how strong the correlation between two signals. If the magnitude is close to 1, it means 2 signals have strong coherency. On the other hand, if the value close to 0, the 2 signals weakly correspond.

In the application of PMU placement for mode shape identification, the generator frequency signals are analyzed. Based on the experience of author, the coherence group of generators are usually formed by several generators connected at the same bus. The magnitude of square coherency function for the generators at the same bus is often close to 1 along the frequency of interest. It indicates that the generators are close electrically and thus it is unnecessary to measure frequency for every single generator.

As an illustration the analysis, the square coherency function is used to identify the generators that are coherence with generator 1. The result is given in the Figure 6.5. It can be concluded that generator 9 is coherence with generator 1 along frequency of interest with the value almost constant equal to 1. Other generators are not coherence with generator 1 since the coherence square values are significantly smaller than 1. Having this result, the measurement can be taken either from generator 1 or generator 9 without significant result difference.

Other coherence groups of generator can also be detected by similar procedure. The results are summarized in the Table 6.4. It can be identified that coherence group normally consists of several generators connected at the same bus. Each group needs only single PMU measurement.

Table 6.3: Mode extraction results

Signal	Frequency (Hz)	Damping (%)
	0.4288	2.2050
Bus 25 vs 21	0.3153	10.6605
	0.6397	3.1290
	0.3246	8.9516
Bus 45 vs 10	0.6630	4.5654
	0.4247	7.7932
	0.6392	2.4035
	0.4231	3.9885
Bus 22 vs 17	0.3206	12.2341
	0.6581	9.5295
	0.6484	2.0487
	0.6790	6.2295
Bus 24 vs 21	0.4687	19.4645
	0.4126	13.3659

Table 6.4: Generator coherence group

Generator	Coherence with generator	Generator	Coherence with generator
1	9	6	14
2	10	7	15
3	11	8	16
4	12	17	-
5	13	-	-

Finally, the complete PMU locations for real-time monitoring application are presented in the Table 6.5. Overall 10 PMUs are deployed in the 17 machine system. Some PMUs are utilized only for mode shape identification such as PMU at bus 18, 45, 22, 19, and so on. Other PMUs are used both for mode shape identification and mode frequency and mode damping identification such as PMU at bus 24 and 21. While PMU at bus 25 is only used for mode frequency and mode damping identification.

6.3 System Order Selection

The effect of system order selection of MYW algorithm to the identification outcome is presented here. Section 3.3 has extensively elaborated the detail of MYW algorithm, and it can be seen that system order, i.e. M, N, and P, should be selected carefully. M, N, and P denote the order of nominator, denominator, and the number equation used respectively.

In practical application, MYW algorithm, or any other algorithms, should be tuned carefully since the true system order is often unknown in advance. The knowledge and experience of the operator or power system engineer play an important role for the order selection. Table 6.6 presents
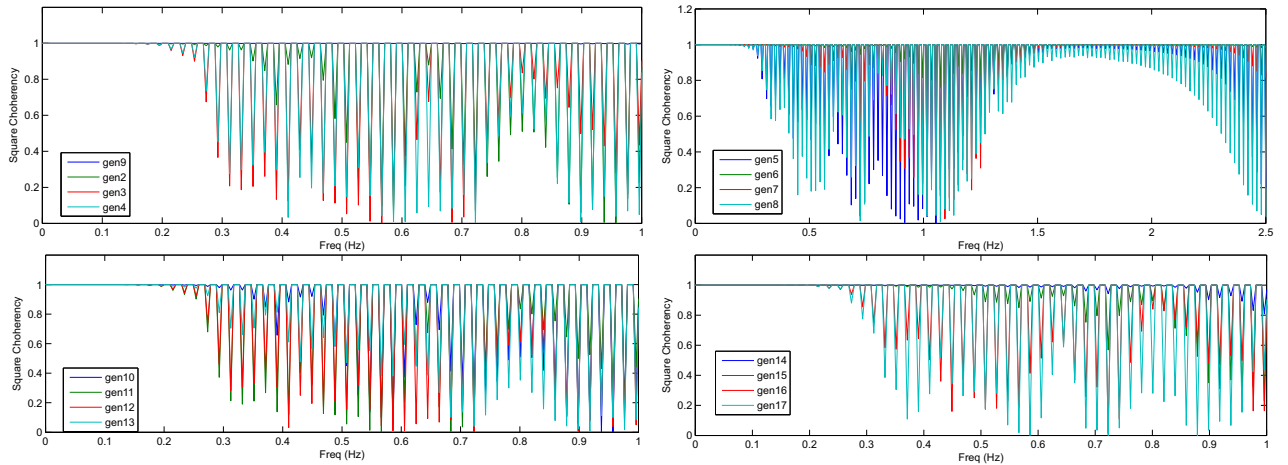
Figure 6.5: Square coherency function with respect to generator 1

Table 6.5: Complete PMU location for 17-machine system

PMU bus	Measurement data	Analysis
17	Bus frequency	Mode shape identification
18	Bus frequency	Mode shape identification
19	Bus frequency	Mode shape identification
20	Bus frequency	Mode shape identification
21	Bus frequency and voltage angle	Mode shape, mode frequency, and mode damping identification
22	Bus frequency	Mode shape identification
23	Bus frequency	Mode shape identification
24	Bus frequency and voltage angle	Mode shape, mode frequency, and mode damping identification
25	voltage angle	mode frequency and mode damping identification
45	Bus frequency	Mode shape identification

various order selection for 17 machine system. The order M=10, P=25, and N=25 provides most reasonable result among the presented order. Therefore, it is selected for mode frequency and mode damping identification in real-time monitoring application. Note that the system order remains the same as long as the system structure also remain the same.

6.4 Test Procedure

The testing conditions need to be performed in order to study the performance of real-time monitoring system under various conditions. The test is necessary to measure the reliability and the accuracy of the application when facing various conditions in power system operation such as abrupt load changes. The testing condition set up is illustrated by Figure 6.6.

According to Figure 6.6, the first step is to prepare the test system and real-time monitoring system, i.e. the offline study. It is also necessary to set up several testing scenarios. The testing scenarios consists of four conditions. First, the ambient condition is used to test the monitoring system under normal operation of power system. Second, the ringdown condition is performed to

Table 6.6: System order selection

System Order	Frequency (Hz)	Damping (%)	System Order	Frequency (Hz)	Damping (%)
M=0,*P*=40, *N*=20	0.4313	5.2004	*M*=10, *P*=40, *N*=20	0.4310	1.8225
	0.3004	8.4616		0.3158	10.1540
	0.6415	4.3802		0.6395	3.1556
	0.6556	4.5876		0.6542	3.9728
M=0,*P*=40, *N*=25	0.4323	4.2441	*M*=10, *P*=40, *N*=25	0.4308	1.7623
	0.3051	7.9276		0.3154	10.2258
	0.6357	3.6309		0.6397	2.97085
	0.6558	4.4587		0.6516	4.9221
M=0,*P*=40, *N*=30	0.4320	3.9008	*M*=10, *P*=50, *N*=25	0.4303	2.0733
	0.3075	7.4765		0.3156	9.9595
	0.6337	3.6961		0.6397	2.7991
	0.6550	4.6020		0.6761	8.6816
M=5,*P*=40, *N*=20	0.4313	2.6604	*M*=10, *P*=60, *N*=25	0.4288	2.2050
	0.3135	8.2086		0.3153	10.6605
	0.6358	4.2125		0.6397	3.1290
	0.6542	3.9728		0.6790	6.2295

test the monitoring system under disturbance condition. Power system often deals with disturbance therefore it is important to test the system under ringdown condition. The third condition examines the ability of real-time monitoring system in giving the recommendation actions to the operator to improve low damping mode. This is performed for both ambient and ringdown condition. The last scenario is to change operating condition in order to measure the ability of real-time monitoring system to track the mode change due to the changing in operating condition. In practical power system, the last condition often changing due to changing in generator and/or load power.

Once the test system, real time monitoring system, and testing scenarios have been prepared, the real-time monitoring can be performed. The real-time monitoring system will provide continuous results about system's inter-area modes. The results of modal properties identification will be compared to modal analysis to check the accuracy. Whereas, the operator recommendation program will be tested with the results of modal sensitivity. It is carried out for ambient condition, ringdown condition, and changing operating conditions.

Section 6.4.1 presents the scenario for monitoring the performance of real-time monitoring system under ambient condition. Under this condition the system is perturbed only by small random load changing. Section 6.4.2 discusses the scenario for testing the real-time monitoring system under ringdown condition. This condition intends to simulate large and sudden change in system. Meanwhile, the ability of real-time monitoring system in improving the damping is tested in Section 6.4.3. Finally, The scenario for examining the change of operating condition is given in Section 6.4.4. The detail of each scenario is discussed in detail in the following sections.
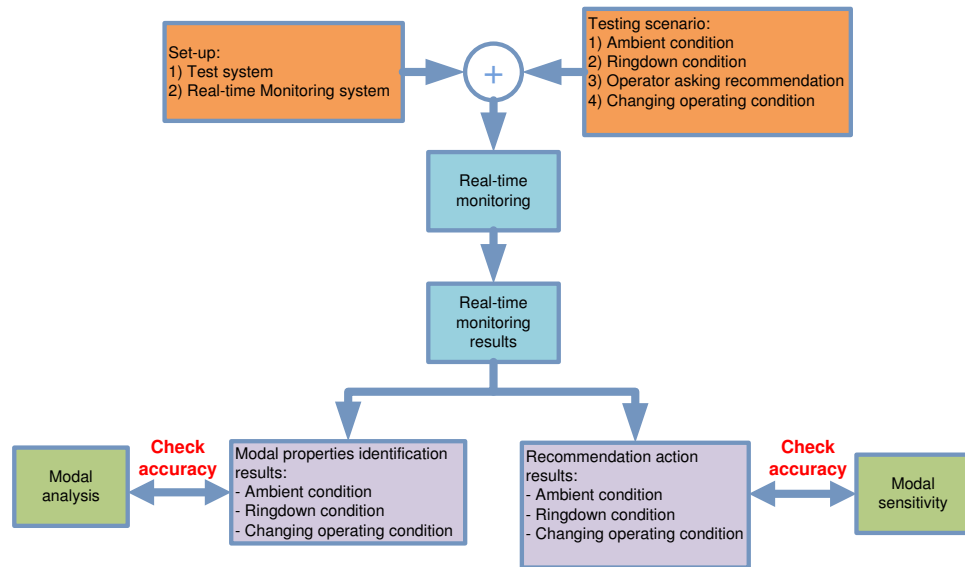
Figure 6.6: Testing condition

6.4.1 Ambient Condition

Ambient data is produced during ambient condition of power system. It happens when power system is in normal operation state under random small load changing perturbation. In this thesis, small random load changing is simulated by passing low pass filtered white Gaussian noise to all active and reactive load. This representation is enough to resemble small random load changing in real power system [12]. Butterworth IIR low pass filter is used in this step by invoking Matlab built-in function *butter*. The filter order is 9 and cut-off frequency is set to 1 Hz.

6.4.2 Ringdown Condition

Section 6.4.1 explained only the scenario under ambient condition. However in practical application, system often encounters with large disturbances and it causes the system generates ringdown data. As previously explained, the basic assumption of the algorithm used in the real-time monitoring application is that the system is perturbed by small random load changing or ambient condition. The real-time application should be able to withstand against ringdown condition. If the application fail, the operator will not be able to see the system condition. Due to this reason, failure in monitoring is totally unacceptable.

In order to generate the ringdown data, 700 MW and 1400 MW load pulse are applied to the system [15]. The load pulse is inserted to bus 35 at t = 700 second and it has 0.5 second duration. As a result, ringdown data will be generated by the power system and real-time monitoring system should be able to pass through this disturbances. The real-time monitoring system is also expected to be able to continuously provide the identification results and recommendation to the operator.

6.4.3 Operational Recommendation

Power system condition is continuously changing due to the constant changing in loads, generations, disturbances, and so on. Therefore, the power system inter-area stability is not constant either. In some occasions, the system stability condition is very strong, but in another occasion, the system can approach to instability. As a result, real-time monitoring application is required. When the system is close to instability, or the inter-area modes with low damping is detected, the real-time application should be able to provide recommendation action to the system operator. It is required to improve the damping of inter-area modes.

In the past, power system operator could improve the inter-area damping based on their experience. However, experience–based actions may not be the most effective choice to improve the damping. Moreover, it can instead degrade the stability condition if incorrect action is taken. Therefore, operator recommendation action is necessary to obtain most effective and secure action. Operator recommendation works based on the principle of modal sensitivity discussed in the Section 3.5. The moda sensitivity will give the most effective generator pair to improve the damping.

To improve the damping of inter-area oscillation, modal sensitivity works differently from Power System Stabilizers (PSS). PSS tries to manipulate control signal and at the same time maintain the same operating condition. In contrast, modal analysis works by adjusting the operating point to more secure condition. Modal sensitivity can also be carried during real-time monitoring. Therefore, it is the advantage of this technique.

In order to measure the ability of modal sensitivity in giving the recommendation action to the operator, this section will set up several simulation scenarios. First, the ability of modal sensitivity to give recommendation during ambient condition is tested. it is to represent modal sensitivity ability during normal operating condition. Second, the scenario is to perform the modal sensitivity during ringdown condition by inserting 700 MW load pulse similar to that of in Section 6.4.2. The result will be compared to the result from modal sensitivity in Figure 6.2 to check the consistency.

6.4.4 Robustness under Changing Operating Condition

This section presents the scenario when the power system changes the operating condition. Practical power system often experiences not only temporary disturbances, but also permanent disturbances. Permanent disturbances normally shifts the operating condition to new operating condition. It includes the conditions when the generator and load changes their power, fault at transmission lines, etc. This makes the inter-area oscillation modes changes as well. Thus, the real-time monitoring system should be able to continuously track the modes changing.

In order to simulate this conditions, the load is represented as step load changing. It is applied to all real loads with the step magnitude is 1%. This means the load will increase by 1% from its previous values. It shall cause the power system to move to new operating condition. The real-time monitoring

will track modes changing during this conditions. The results from both old operating condition and new operating condition are compared to result's of modal analysis taken from respective operating condition.

CHAPTER VII

TEST RESULTS

The performance results of real-time monitoring against various scenario, previously presented in Section 6.4, are analyzed. The important results are discussed. Section 7.1 analyzes the result against ambient condition. The performance of inter-area monitoring under the ringdown data is also pointed out in Section 7.2. Section 7.3 discusses about the ability of mode sensitivity to obtain recommendation action to the operator. Finally, The results during operating condition changing are given in Section 7.4.

7.1 Performance under Ambient Condition

Under ambient condition, system is perturbed by random small load changing. It can be done by passing low filtered white noise to both real and reactive load. This filter is often termed as $1/f$ filter or pink noise. The result of this perturbation is ambient response in power system variables such as generator speed, generator output, power flow, and so on. The example of ambient signal is depicted in Figure 7.1 showing one minute voltage angle difference between bus 25 vs 21 in radian unit.

Table 7.1: Modal analysis vs real-time identification

Modal Analysis		Real-time monitoring at t=630.221 s	
Frequency (Hz)	Damping (%)	Frequency (Hz)	Damping (%)
0.3179	10.7394	0.3179	11.1205
0.4219	3.6275	0.42556	3.1031
0.6349	3.9370	0.6400	3.8967
0.6730	7.6347	0.6751	5.9383

For real-time monitoring, the windows length is set to 10 minutes. The real-time monitoring system should be initiated with artificial ambient data having the same characteristic as that of ambient data described in section 6.4.1. Therefore, the system will convergence after the time reaches 10 minutes or 600 second. Figure 7.2 presents the graph in GUI as system initiated by artificial ambient data. The artificial ambient data is encircled by blue box whose data length is equal to 550 second and the real ambient data, encircled by magenta box, has 50 second data length. Real ambient data is produced by the monitored power system. The artificial ambient data keeps being discharged as the real ambient data continuously grows. After 600 second, all artificial ambient data will be completely discharged. Thus, artificial data is no longer used in the real-time monitoring.

As shown by Figure 7.3, the monitoring system contains all ringdown data from the simulated power system, and no artificial ambient data exists. The result of mode damping and mode frequency
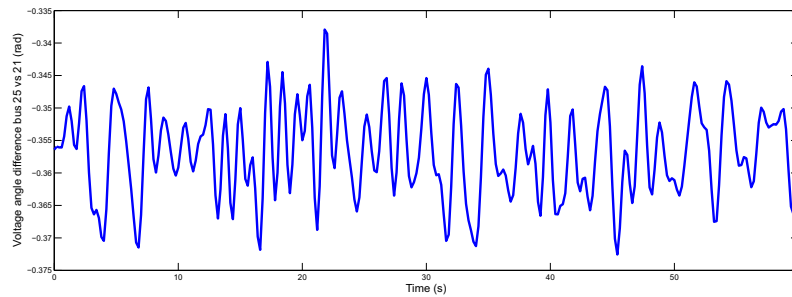
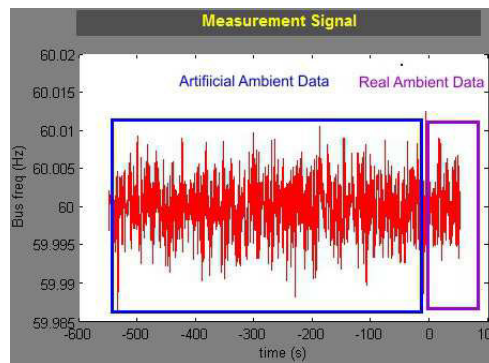Figure 7.1: Voltage angle difference between bus 25 vs 21

Figure 7.2: Plot in GUI with artificial ambient data

at t= 630.221 second is also obtained. If one compare the result with modal analysis in Table 6.1, it can be drawn a conclusion that the result is accurate enough. Table 7.1 summarizes the comparison between modal analysis and real-time monitoring result at t= 630.221 second. It can also be observed that the identification result of mode frequency is more accurate than the identification result of mode damping. The mode damping identification is much more sensitive to the presence of noise in the data than that of frequency damping identification. The modes can also be plotted in s-plane to graphically monitor its dynamic. In Figure 7.3, there are two modes located in the red area whose the damping is between 0– 5%, one mode in yellow area with the damping is between 5–10% and one mode green area whose the mode is between 10–20%.

Figure 7.3 also shows mode shape of 2nd mode with frequency 0.42556 Hz. The result is provided in the form of both table and graphic representation. The result indicates that mode 0.42556 Hz is a main interaction between northern half vs southern half and bus 45 of 17 machine system. Bus 18, bus 45, and bus 19 are the most participated bus in this swing mode. Bus 18, bus 17, and bus 22 swings against bus 45, bus 19, and bus 20. The accuracy of the result can be directly verified by comparing with Table 6.2. Table 7.2 summarizes the comparison mode shape of mode 0.4219 Hz from modal analysis and real time monitoring. It can be concluded that the result from real-time monitoring is accurate. The difference, also the case for mode frequency and mode damping, is likely caused by the different basic approach of those two methods. Modal analysis is a static analysis, and it
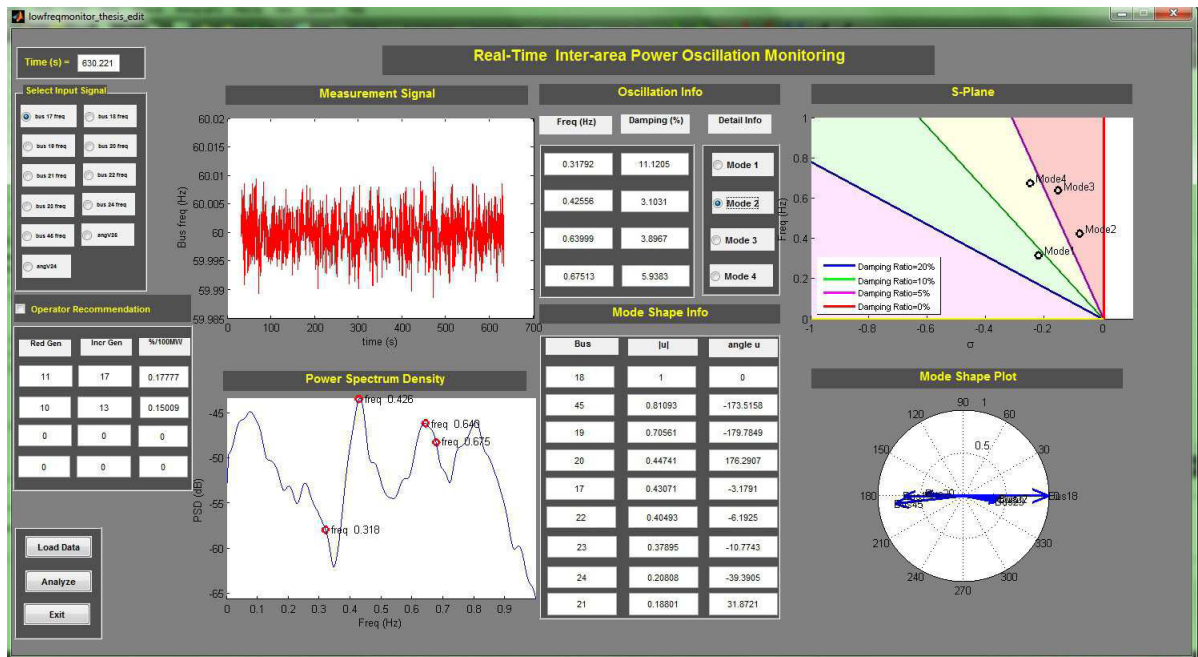
Figure 7.3: GUI appearance with mode shape of 0.42556 Hz mode

assumes that the operating condition is constant. While, real-time monitoring uses data from ambient data which is indeed non-constant. Moreover, to obtain modal properties, real-time monitoring needs 0.569385 seconds for one operating condition and it is much faster compared to modal analysis's time requirement i.e. 2.828788 seconds.

The operator can change what is displayed in the GUI simply by clicking either the corresponding PMU signal's name or mode's name. Changing the PMU name will change the display of moving window and the PSD of corresponding signal. Meanwhile, changing the mode name will change the mode shape corresponding to that mode. It happens for both table representation and plot representation. Figure 7.4 depicts the GUI appearance with operator have changed PMU signal and mode shape from previous display in Figure 7.3. In this figure, the voltage angle difference between bus 24 and 21 is selected thus the corresponding moving window plot and PSD change accordingly. The PSD shows that the signal has good observability in the frequency around 0.6 Hz. Figure 7.4 also depicts that the mode shape is turned into mode shape of 0.6365 Hz mode. This mode, based on modal analysis in Table 6.1, is main interaction of bus 20 and bus 21 against bus 24. The mode shape table and mode shape plot in GUI confirms this result.

Under ambient condition, the stability condition of the system is relatively constant every time. Although the system is perturbed continuously, it is just small fluctuation around the stationary operating point. Thus, there is no significance shift in the stability condition. It can be checked by studying the mode frequency and mode damping of inter-area modes at different time interval. Suppose one checks the stability condition at t = 810.287 second. The result of mode frequency and mode damping from real time monitoring is given in the Table 7.3. If this result is compared with
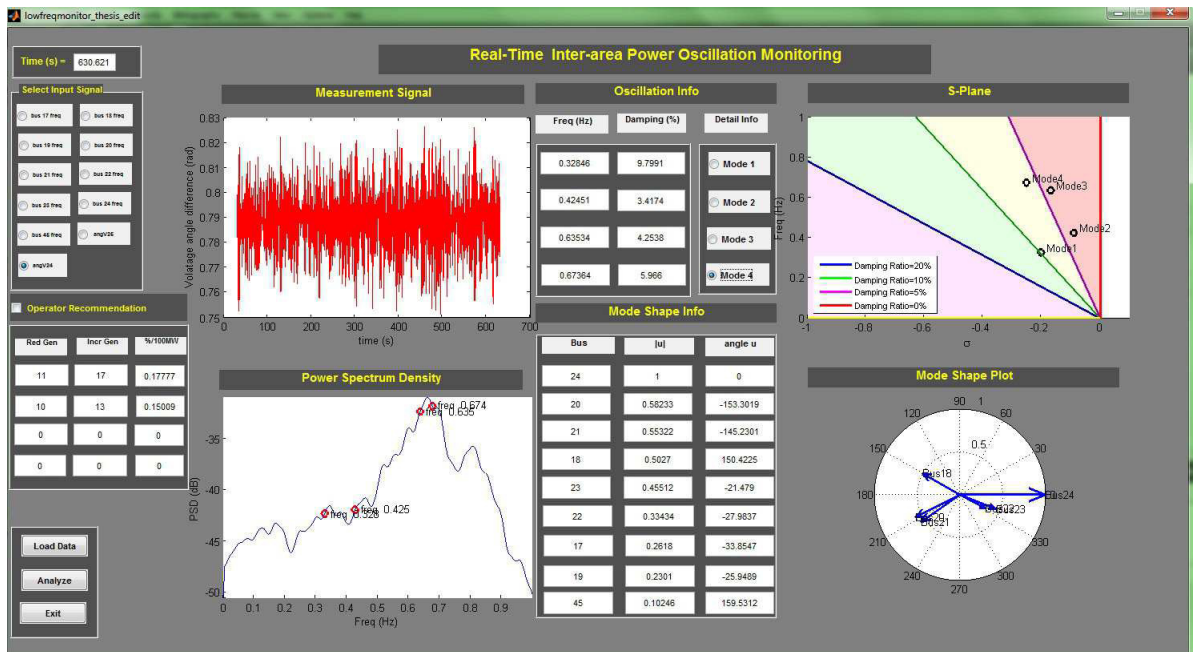
Figure 7.4: GUI appearance with different signal display

with previous result at t = 630.221 second, they are not significantly different. The mode frequency is relatively constant, but the mode damping changes by small amount. Mode frequency is relatively constant as long as system structure is still constant. In contrast, the damping can change because the generation and load continuously change.

7.2 Performance under Ringdown Condition

Power system under ambient condition can be suddenly excited due to an abrupt change in power system variables such as large disturbance and rapid change of large load. Many disturbances in power system can be usually categorized as instant or temporary disturbance. In other words, it may be categorized as pulse disturbance. When system is experiencing large disturbance, the protection system tends to remove the disturbance as quick as possible to avoid system instability. It can be interpreted as instantaneous disturbance from power system point of view. Such condition is called ringdown condition, and it is characterized by strong oscillation in power system measurement. Under this conditions, real-time monitoring system should not fail working. It should also be able to provide accurate information about the system stability status and also capable of providing an accurate recommendation action for the system operator.

In order to measure the ability of real-time monitoring system to withstand the ringdown condition, two standard load pulses, i.e. 700 MW and 1400 MW, are applied to the power system [15]. The duration of the load pulse is set to 0.5 second. Bus 35 is selected as the location to inject the load pulse as being explained in section 6.4.2. The power system will experience ambient condition

Table 7.2: Mode shape of 0.4219 Hz mode: modal analysis vs real-time calculation

	Modal Analysis		Real-time monitoring at t=630.221 s	
Bus	$|u|$ (normalized)	$\angle u$	$|u|$ (normalized)	$\angle u$
18	1.00	0	1	0
45	0.8569	-183.1249	0.81093	-173.516
19	0.5959	-168.6048	0.7056	-179.7845
17	0.4305	-0.8470	0.43071	-3.1791
22	0.4007	-2.5455	0.40493	-6.1925
23	0.3786	-7.2351	0.37895	-10.7743
20	0.3727	-167.8277	0.44741	176.2907
24	0.1507	-21.9713	0.20808	-39.3905
21	0.1404	13.5787	0.18801	31.8721

Table 7.3: Inter-area modes at t= 810.287 s

Frequency (Hz)	Damping (%)
0.32288	11.3526
0.4209	3.0323
0.63842	4.275
0.66562	5.9295

first, and at t = 700 second the load pulse is injected to produce ringdown condition. The performance real-time monitoring to monitor system condition is measured during three different time intervals i.e. prior load pulse is applied, during the pulse is applied, and post the load pulse is applied. The 700 MW load pulse is applied first. Using the same scenario, the 1400 MW load pulse is applied after the first load pulse is applied. Figure 7.5 gives an example of ringdown response of frequency at bus 17 after 1400 MW load pulse is applied to the bus 35 at t= 30 second. According to the figure, the difference between ambient response and ringdown response is obvious. Ringdown response is characterized by strong oscillation from t = 30 second to t = ± 60 second. Whereas, the ambient data is characterized by random load changing with small oscillation.

The performance of real-time monitoring during the insertion of 700 MW load pulse is discussed first. Prior to the insertion of load pulse, the monitoring system operates normally and provides accurate information regarding the inter-area oscillation in the power system. The screen shot of GUI monitoring system prior to the disturbance is given in the Figure 7.6. Since this condition is ambient, the result is not significantly different from the result in section 7.1. At t = 700 second, the 700 MW load pulse is inserted at bus 35. The ringdown response is produced, and it is captured by GUI as shown in the Figure 7.7. The presence of ringdown signal does not cause failure to real-time monitoring application and moreover it does not significantly affect the capability of real-time
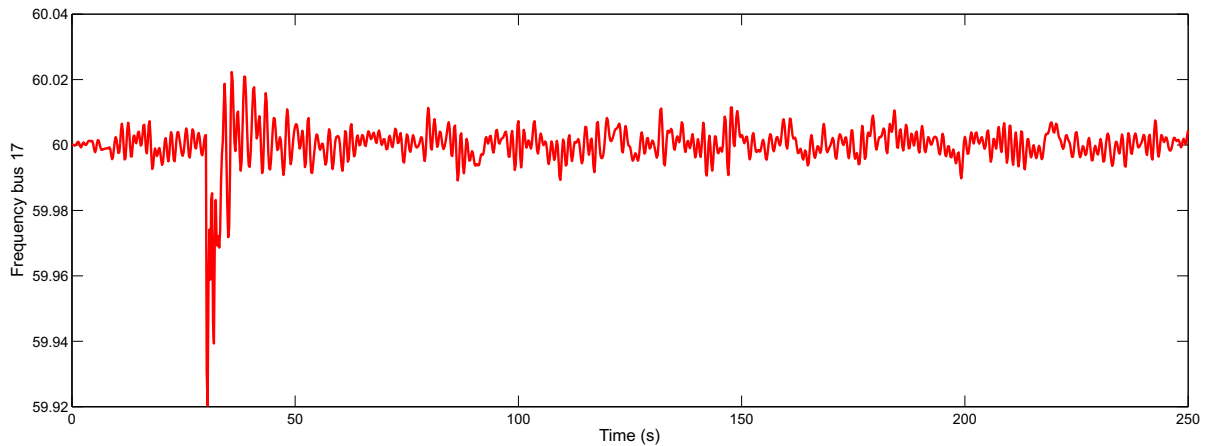
Figure 7.5: Frequency of bus 17 during ambient and ringdown condition

monitoring results.

After several minutes, the system condition returns to ambient condition. The data containing ringdown response is no longer used for identification. This result is given in the Figure 7.8 and it is not significantly different from that of in the Figure 7.6 and 7.7. Some modes have a lower damping than the damping before load pulse insertion. While, others have higher damping damping than that of prior to load pulse insertion. It may be caused by the insertion of load pulse which shifts some parameters to new operating point. In addition, the value of mode frequency is relatively more constant than the value of damping.

Table 7.4: Mode change for 1400 MW load pulse

Prior insertion		During insertion		Post insertion	
Frequency (Hz)	Damping (%)	Frequency (Hz)	Damping (%)	Frequency (Hz)	Damping (%)
0.34781	12.0485	0.29636	12.4089	0.32674	8.9405
0.43068	2.8717	0.42581	3.0254	0.42104	3.1066
0.6385	3.1069	0.63675	3.8482	0.62895	3.5466
0.66667	4.7297	0.6552	6.1942	0.69966	3.3617

A 1400 MW load pulse is also applied to the system. Note that the size of the load pulse is twice the first load pulse and it may cause severe problem to monitoring system. The result is then also monitored at three different intervals i.e. prior load pulse is applied, during the pulse is applied, and post the load pulse is applied. However, here the GUI screen shot is not provided. The result is given in the form of table i.e Table 7.4 for mode frequency and mode damping and Table 7.5 for mode shape. It can be observed that the real-time monitoring system can still provide accurate results even for larger disturbance. The damping of some mode changes due to the load pulse insertion. Whereas, the mode frequency and mode shape is relatively constant. This is true because, as previously mentioned, mode frequency and mode shape is strongly affected by the system structure. As long as the system does not change significantly, the mode frequency and mode shape will not
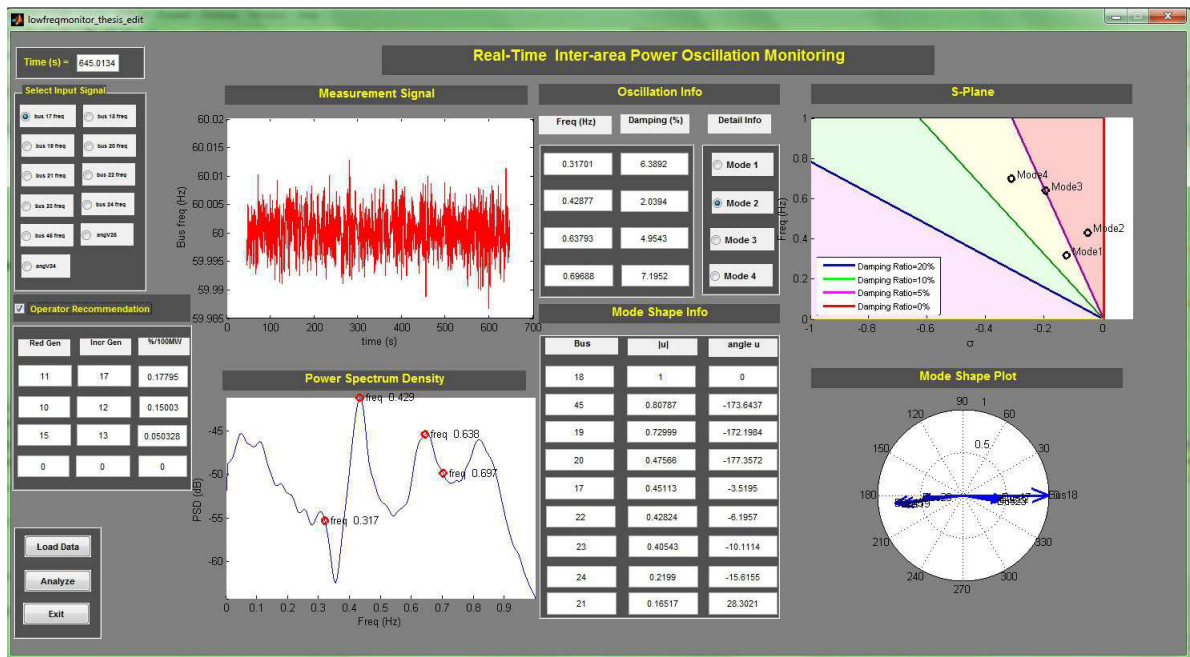
Figure 7.6: GUI appearance prior to 700 MW load pulse insertion
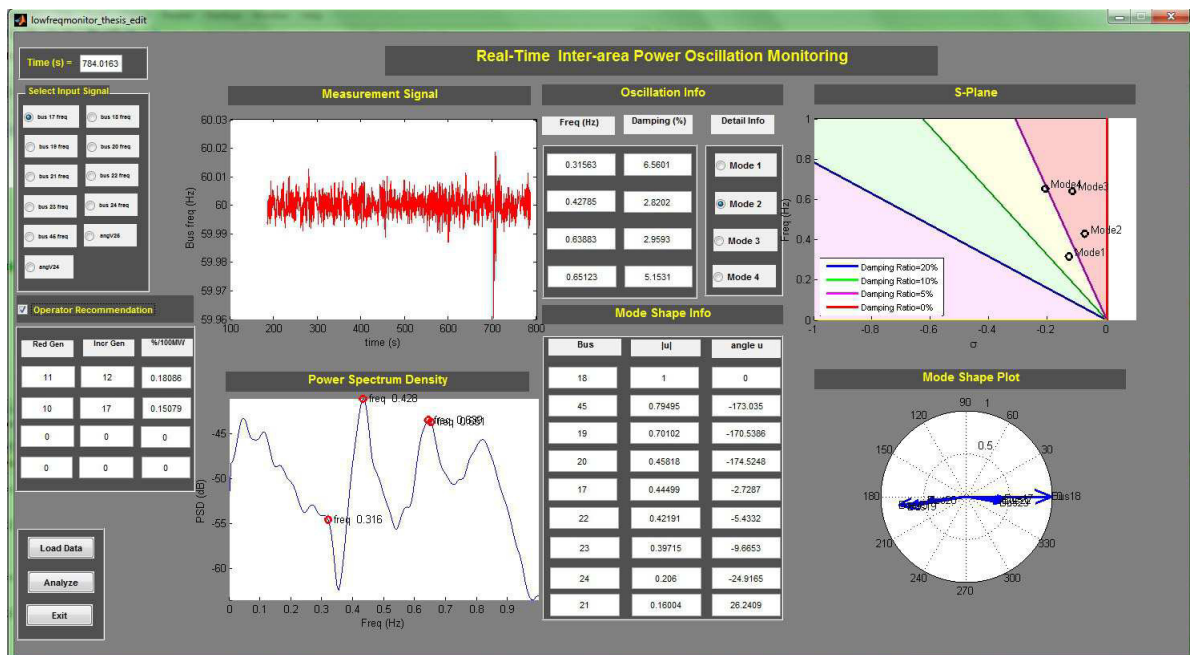
Figure 7.7: GUI appearance during 700 MW load pulse insertion

change significantly. Here, the load pulse does not change the system structure.

Finally, it can be drawn a conclusion that the real-time monitoring system works successfully when the system is under ringdown condition due to the insertion of 700 MW and 1400 MW load pulse. The real-time monitoring is still able to provide accurate information regarding the inter-area oscillation of power system.
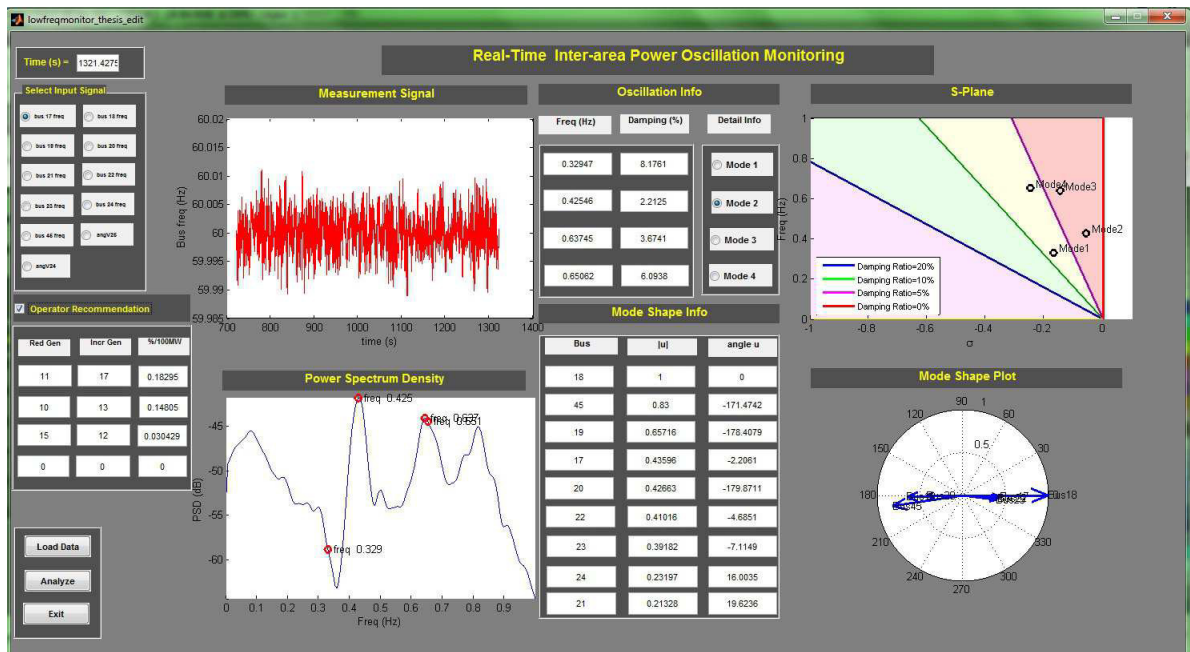
Figure 7.8: GUI appearance post 700 MW load pulse insertion

Table 7.5: Mode shape change for 1400 MW load pulse

Bus	Prior insertion		During insertion		Post insertion	
	$|u|$ (normalized)	$\angle u$	$|u|$ (normalized)	$\angle u$	$|u|$ (normalized)	$\angle u$
18	1.00	0	1	0	1	0
45	0.8002	-172.485	0.815	-168.23	0.873	-173.89
19	0.686	-177.78	0.649	-170.01	0.615	-172.78
17	0.450	-0.2056	0.429	1.96	0.432	-3.78
22	0.425	-4.89	0.405	-1.11	0.406	-7.08
20	0.418	176.025	0.402	-176.19	0.405	-179.13
23	0.397	-9.23	0.378	-6.07	0.39	-12.7
21	0.2302	-27.67	0.184	32.86	0.218	29.5
24	0.197	-19.335	0.1815	-31.2454	0.25	-40.01

7.3 Performance of Operational Recommendation

The presence of operator recommendation in real-time monitoring is very essential for power system operator. The operator recommendation gives a list of actions to improve the low damping mode. It is established on the concept of modal sensitivity discussed intensively in section 3.5. Operator recommendation works by redispatching the generator power output to move to more secure operating point, and it is always come as a pair of action. Improving a generator output should be rebalanced by reducing another generation output to maintain the balance of generation and load.

Table 7.6: Recommendation list during ambient condition

Reduce generator	Increase generator	Expected damping improvement (%/100 MW)
11	17	0.1893
10	13	0.1454
14	12	0.022949

However, power system operation often encounters with disturbances such as change of large load, short circuit, generator trip, an so on. It results strong and large oscillation in power system variables. In this condition, real-time monitoring should still be able to provide the correct recommendation to the system operator. Incorrect recommendation may deteriorate the system condition.

This section will perform the simulation according to the scenario in section 6.4.3. The result will be discussed and important finding will be underlined. First, the ability of operator recommendation under the ambient condition is tested and the results are then compared to modal sensitivity result in section 6.1 for validation. In addition, the result can also be validated using modal analysis by changing the generation based on the recommendation list and calculate the damping improvement.

Second, the ringdown condition is considered, and the operator recommendation is tested during this condition. The ringdown condition is generated by inserting 700 MW load pulse at t = 800 s. Bus 35 is selected for inserting the load pulse. The result is validated using the same procedure as that of ambient data.

To begin with, the ambient condition is discussed first. The ambient data is generated using random load having the same characteristic as that in section 7.1. To illustrate, the 0.4219 Hz mode in Table 6.1 is selected as a mode of interest since it has the lowest damping among other modes. Thus, the goal is to acquire a recommendation lists for improving the damping of 0.4219 Hz mode. The result is given in the Figure 7.9. In addition, Table 7.6 provides list of recommendation in form of table. According the recommendation from real-time monitoring application, the most effective pair for improving the damping of 0.4219 Hz mode is generator 11 and 17. By reducing the output of generator 11 and at the same time, increasing the output of generator 17, it is expected that the mode damping will increase rate around $^{0.1893\%}/_{100\ \mathrm{MW}}$. However the expectation value may not represent true rate when the corresponding pair is selected. In order to check the validity of the first choice, one can compare with the result given in Figure 6.2. Base on the figure, the generator 11 and 17 also make up the most effective pair whose the slope difference is the largest among other choices. The slope difference is around $^{0.1134\%}/_{100\ \mathrm{MW}}$, and it is different from the result of operator recommendation application.

In the same way, the operator recommendation also suggests that another generator pair i.e. generator 10 and generator 13 can be picked up to improve the damping of 0.4219 Hz mode. Reducing the output of generator 10 and increasing the output of generator 13 at the same amount will produce the estimated mode increment around $^{0.1454\%}/_{100\ \mathrm{MW}}$. To check the validity of the pair, one can again
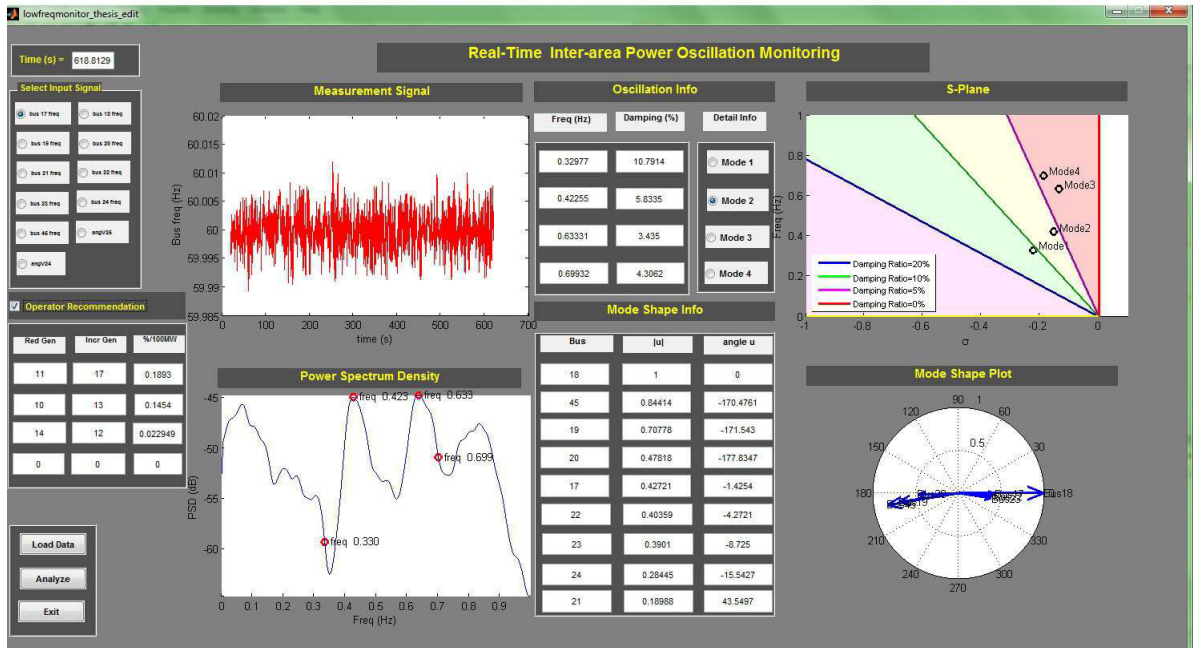
Figure 7.9: GUI appearance for operator recommendation under ambient condition

compare this recommendation to Figure 6.2. It can be drawn a conclusion that the result from both approaches is consistent, and it validates the operator recommendation application approach.

Furthermore, the validation can also be carried out by calculating the modal analysis of the system after changing the generation pair based on the recommendation. The result is then compared with the base case whose the modes are shown in Table 6.1. After that, the damping changes is calculated. The result is summarized in the Table 7.7. Note the here all generators are increased or reduced by one p.u. The result shows that the order of damping increment from the basic case is in the same order as that in the operator recommendation. Table 7.7 also confirms the validity of the last recommendation, i.e. reducing generator 14 and increasing generator 12, since it cannot be done using Figure 6.2.

A deeper analysis also concludes the recommendation often consists of generators with relatively high participation to that particular mode. In other words, there is a relationship between the generator appearing in recommendation list and the participation of bus in oscillation mode. Comparing Table 7.2 with Table 7.6, it can be concluded that generator 11, 17, 10, and 14 are located in the bus having relatively high participation to the 0.4219 modes. Like in case of PSS, generator with high participation in mode of interest is often selected as PSS location candidate. Similarly, here the generators with high participation in a mode often show up as a recommendation list for redispatching the power flow.

In contrast, the absence of operator recommendation may lead inappropriate action by the system operator. Consequently, it can result unfavorable system condition such as decrements of mode damping. Suppose, the operator take opposite actions from that in Table 7.7 in order to improve

Table 7.7: Damping change of 0.4219 Hz mode

Case	Damping (%)	Damping change from base case (%)
Basic	3.6275	0
reduce gen 11, increase gen 17	3.7091	0.0816
reduce gen 10, increase gen 13	3.6659	0.0384
reduce gen 14, increase gen 12	3.6336	6.1×10^{-3}

Table 7.8: Damping change of 0.4219 Hz mode with incorrect action

Case	Damping (%)	Damping change from base case (%)
Basic	3.6275	0
increase gen 11, reduce gen 17	3.5486	-0.0789
increase gen 10, reduce gen 13	3.5884	-0.0391
increase gen 14, reduce gen 12	3.6209	-6.6×10^{-3}

the damping condition. The result is presented in Table 7.8. It could be underlined that inappropriate actions decrease mode damping instead of improving it. It is arguably unfavorable condition for power system, and in extreme case, major system black out may follow immediately.

The explanation above has demonstrated that the operator recommendation program in real-time monitoring application can work well during the normal or ambient condition. Nevertheless, power system often experiences with large disturbance, and it causes ringdown response in power system variables. Under ringdown condition, real-time monitoring should prevail the ability to obtain appropriate recommendation list to the system operator.

To measure the ability of real-time monitoring system to provide list of operator recommendation, the 17 machine system is perturbed with 700 MW load pulse at t = 800 s. The bus 35 is again selected to inject the load pulse. During the presence of ringdown data, the GUI screen shot is given in the Figure 7.10, and the list of recommendation is provided in Table 7.9. By observing the recommendation, it can be drawn a conclusion the real-time monitoring system is still able to give a list recommendation to system operator. The result of recommendation is also similar to that of during the ambient condition.

Table 7.9: Recommendation list during ringdown condition

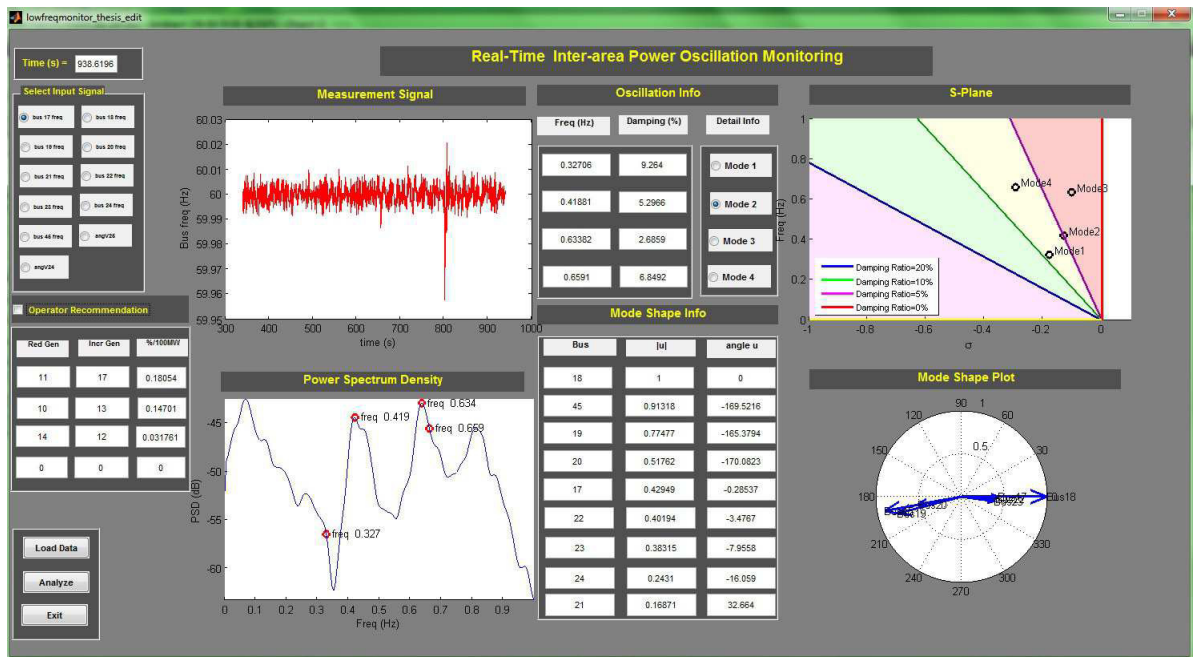| Reduce generator	Increase generator	Expected damping improvement (%/100 MW)
11	17	0.18054
10	13	0.14701
14	12	0.031761

Figure 7.10: GUI appearance for operator recommendation under ringdown condition

7.4 Robust Performance of Changing Operating Condition

Changing operating condition often occurs in practical power system. It can be caused by loading changing, fault, etc. Changing operating condition undoubtedly cause changing in inter-area modes. The real-time monitoring system, therefore, should be able to follow this changing. To perform this condition, all real loads are modeled as step load changing. The loads are increased by 1% from previous value after t = 700 s. The results of mode properties identification and operator recommendation are presented for both before and after changing in operating condition.

Before the changing of operating condition, the result of mode frequency and mode damping identification is given in Table 7.10. Table 7.10 also provides the mode frequency and mode damping from the corresponding modal analysis. It can be drawn a conclusion that the result is very close. Meanwhile, the result for mode shape identification and the comparison with modal analysis are shown in Table 7.11. The result of mode shape identification is also close to that of from modal analysis. It should be noted that the result is given only at t = 662.6275 s.

Table 7.10: Modal analysis vs real-time identification before operating condition changing

Modal Analysis		Real-time monitoring at t=662.6275 s	
Frequency (Hz)	Damping (%)	Frequency (Hz)	Damping (%)
0.3179	10.7394	0.32095	9.8671
0.4219	3.6275	0.42568	3.2745
0.6349	3.9370	0.63765	3.1716
0.6730	7.6347	0.6775	3.7067

After t = 700 s, the operating condition is shifted by introducing step changing in all real loads.

Table 7.11: Mode shape of 0.4219 Hz before operating condition changing

	Modal Analysis		Real-time monitoring at t=630.221 s	
Bus	$\lvert u \rvert$ (normalized)	$\angle u$	$\lvert u \rvert$ (normalized)	$\angle u$
18	1.00	0	1	0
45	0.8569	-183.1249	0.8650	-172.31
19	0.5959	-168.6048	0.7004	-175
17	0.4305	-0.8470	0.433	-2.32
22	0.4007	-2.5455	0.40556	-5.42
23	0.3786	-7.2351	0.382	-10.6532
20	0.3727	-167.8277	0.454	179.8
24	0.1507	-21.9713	0.26326	-37.68
21	0.1404	13.5787	0.21	29.56

Step changing is set to 1% from previous value. The example of GUI appearance during this changing is shown in Figure 7.11. It shows the dynamic of bus 17 frequency, and it can be seen the frequency step changing due to the load changing at t = 700 s. Once the data converges, the result of mode frequency and mode damping is shown in Table 7.12. It shows the result at t = 1567.43 s. While, the result of 0.42 Hz mode shape is shown in Table 7.13. The results show that the real-time monitoring can track the modal properties changing with acceptable accuracy. The GUI appearance after the input data converge is given in Figure 7.12. The list of recommendation actions after operating condition changes is shown in Table 7.14.

Table 7.12: Modal analysis vs real-time identification after operating condition changing

Modal Analysis		Real-time monitoring at t=1567.43 s	
Frequency (Hz)	Damping (%)	Frequency (Hz)	Damping (%)
0.3166	10.6568	0.32853	4.2876
0.4210	3.5727	0.42343	4.3091
0.6341	3.9593	0.63099	4.1074
0.6696	7.6990	0.69081	4.3203
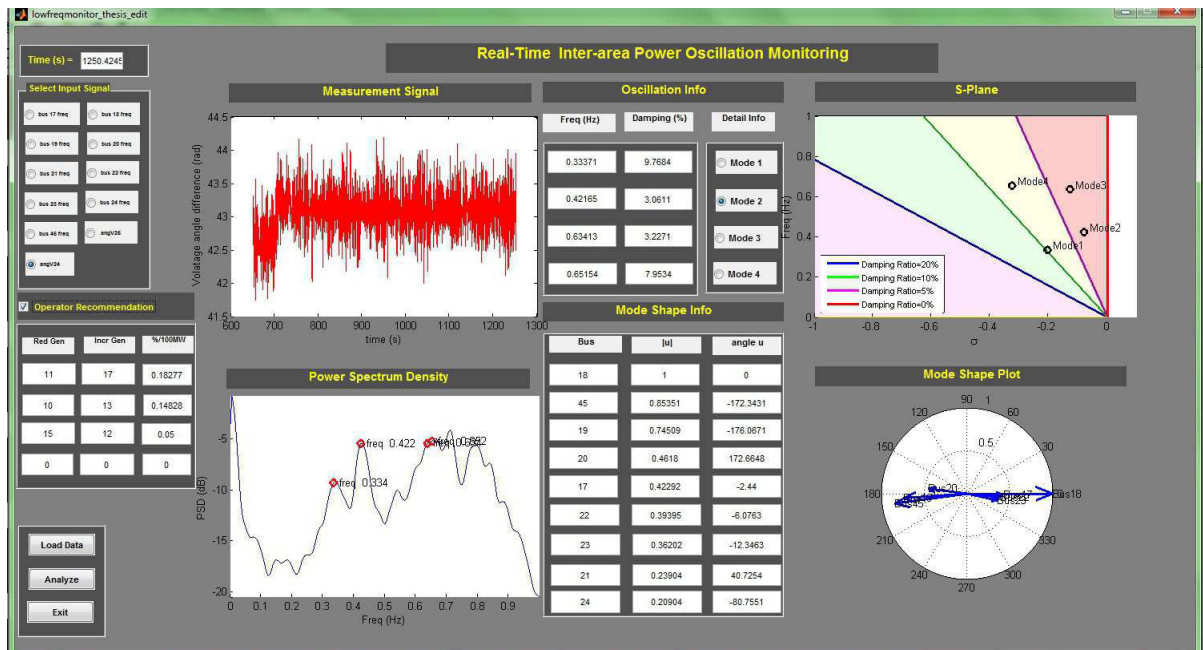
Figure 7.11: GUI appearance during changing operating condition

Table 7.13: Mode shape of 0.4219 Hz before operating condition changing

	Modal Analysis		Real-time monitoring at t=1567.43 s	
Bus	$|u|$ (normalized)	$\angle u$	$|u|$ (normalized)	$\angle u$
18	1.00	0	1	0
45	0.8688	177.1920	0.8667	-173.1
19	0.5943	-169.1919	0.723	-175.54
17	0.4322	-0.7043	0.4378	-2.98
22	0.4021	-2.4434	0.4118	-6.2
23	0.3803	-7.0657	0.386	-11.65
20	0.3650	-168.7068	0.4589	175.87
24	0.1505	-20.3806	0.247	-47.28
21	0.1477	14.8890	0.21	40.95

Table 7.14: Recommendation list after changing operating condition

Reduce generator	Increase generator	Expected damping improvement (%/100 MW)
11	17	0.186
10	15	0.1406
14	13	0.04
16	20	0.02

Figure 7.12: GUI appearance after changing operating condition

CHAPTER VIII

CONCLUSION

8.1   Conclussion

In this thesis, the concept of real-time monitoring of inter-area power oscillation using PMU has been presented. There are some conclusions which can be drawn:

1. PMU placement strongly depends on the type of analysis that is going to be performed. In order to locate PMU for mode frequency and mode damping estimation, the PMU is placed based on the concept of mode obs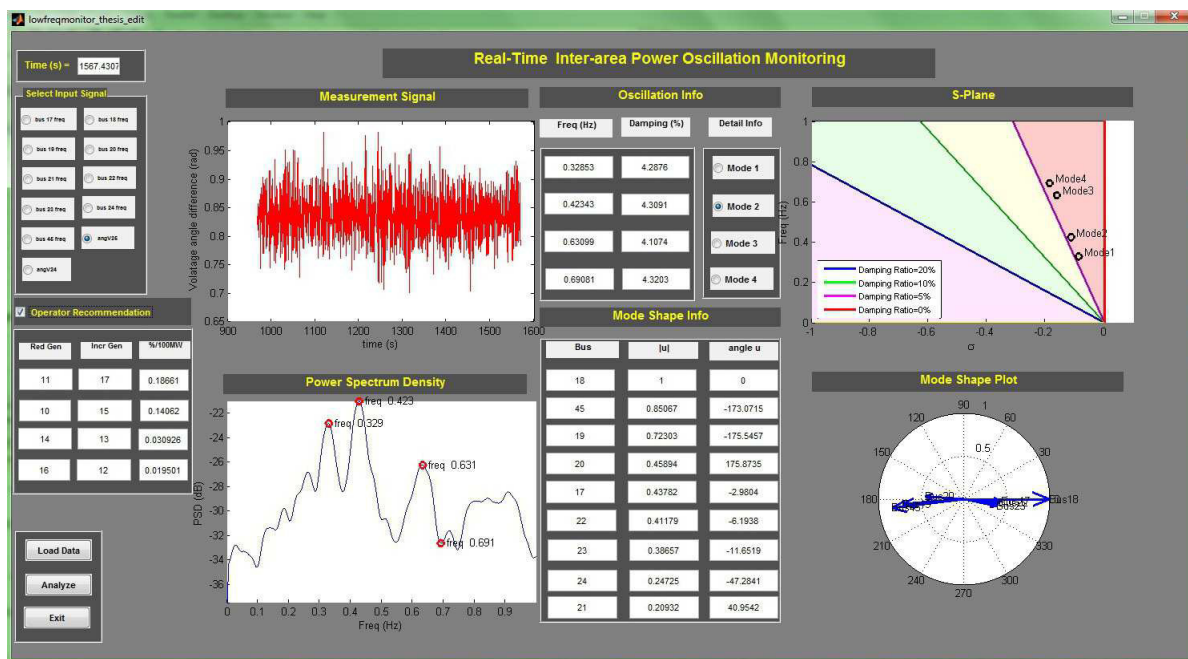ervability in measured PMU signal. The PMU location is selected to the bus whose the signal has high observability. The Observability can be estimated using PSD function. While, to locate PMU for estimating mode shape, the coherency square function is used to classify coherency group of generator. The PMU is located at each coherence group of generator.

2. The mode frequency and mode damping can be accurately identified from PMU measurement. The Modified Yule-Walker (MYW) method is utilized to extract these properties from PMU measurement. Mode damping identification is much more challenging that mode frequency identification due to the fact that mode damping is very sensitive to the presence of noise.

3. Mode shape identification can be estimated using spectral analysis function i.e. Power Spectral Density (PSD) and Cross Spectral Density (CSD). The test demonstrates that mode shape identification can be accurately identified from PMU measurement.

4. The operator recommendation application of real-time monitoring can provide the list of recommendation actions to the system operator to improve the mode with low damping. This method is established on the modal sensitivity analysis.

5. Real-time monitoring system can work well during both ambient condition and ringdown condition. The basic assumption of real-time monitoring program and its features is to work during ambient data. But the test results confirmed that it could also work during ringdown condition without significant difference.

6. Real-time monitoring system requires faster analyzing time to obtain modal properties compared to that of modal analysis. It consumes 0.569385 seconds which is much faster than time of modal analysis i.e. 2.289441 seconds.

8.2 Future Work

Some factors can be taken into account in order to improve this research. Some suggestions for future work are:

1. *Use the shorter data length for identification*

   The data length in this research is set to 10 minutes. Since if shorter data length is used, the MYW methods is unable to provide accurate result of identification. As a result, the identified result less represents the current system condition. It is caused by the nature of MYW to put equal weight to all data. More recent data should be given more weight that the older one. The longer data also means that in case the incorrect data enters data window , it takes longer time to spill out it.

2. *Use online self-tuning identification technique*

   In this research, the MYW method is tuned offline. As a result, when the system structure changes significantly, the MWY will not be able to provide accurate result. It is because the tuning is for old system structure. Self-tuning algorithm is able to adapt its parameters to system structure's change.

3. *Implementation to real power system*

   All the results presented in this thesis is based on simulated data. To measure the effectiveness to practical power system, the real-time monitoring system should be implemented to practical power system as well.

REFERENCES

[1] Klein, M., Rogers, G. J., and Kundur, P. A fundamental study of inter-area oscillations in power systems. in <u>IEEE Transactions on Power Systems</u> 6, 3(August 1991) : 914–921.

[2] Rogers, G., <u>Power Systems Oscillations</u>.London: Kluwer Academic, 2000.

[3] Kundur, P., <u>Power system stability and control</u>. 4, New York: McGraw-Hill, 1994.

[4] Ning, Z., Pierre, J. W., and Hauer, J. F. Initial results in power system identification from injected probing signals using a subspace method. in <u>IEEE Transactions on Power Systems</u> 21, 32006 : 1296–1302.

[5] Ning, Z., Pierre, J. W., Trudnowski, D. J., and Guttromson, R. T., Robust RLS Methods for Online Estimation of Power System Electromechanical Modes. in <u>IEEE Transactions on Power Systems</u> 22, 3(2007) : 1240-1249.

[6] Ning, Z., Trudnowski, D. J., Pierre, J. W., and Mittelstadt, W. A. Electromechanical Mode Online Estimation Using Regularized Robust RLS Methods. in <u>IEEE Transactions on Power Systems</u> 23, 4(2008) : 1670-1680.

[7] Ning, Z., Zhenyu, H., Tuffner, F., and Shuangshuang, J., Automatic implementation of Prony analysis for electromechanical mode identification from phasor measurements. in <u>Power and Energy Society General Meeting, 2010 IEEE</u>, pp.1–8, July 2010.

[8] Trudnowski, D.J. Estimating electromechanical mode shape from synchrophasor measurements. in <u>IEEE Transactions on Power Systems</u> 23, 3(2008) : 1188–1195.

[9] Eissa, M.M., et al., A Novel Back Up Wide Area Protection Technique for Power Transmission Grids Using Phasor Measurement Unit. in <u>IEEE Transactions on Power Systems</u> 25, 1(January 2008) : 270–278.

[10] Phadke, A.G. and Thorp, J.S., <u>Synchronized Phasor Measurements and Their Applications</u>. New York: Springer, 2008.

[11] Trudnowski, D., Donnelly, M., and Lightner, E., Power-System Frequency and Stability Control using Decentralized Intelligent Loads. in <u>Transmission and Distribution Conference and Exhibition, 2005/2006 IEEE PES</u>, pp.1453–1459, May 2006.

[12] Hauer, A.J.F., et al.,A Perspective on WAMS Analysis Tools for Tracking of Oscillatory Dynamics. in <u>Power Engineering Society General Meeting, 2007. IEEE</u>,pp. 1–10, June 2007.

[13] Padiyar, K., R., <u>Power system dynamic stability and control</u>. 2, BS Publications, 2008.

[14] Pal, B., Chaodhuri, B., <u>Robust control in power system</u>. New York: Springer, 2005.

[15] Messina, A., R., <u>Inter-area oscillation in power system: A nonlinear and nonstationary perspective</u>. New York: Springer, 2009.

[16] Chung, C.Y., et al., Probabilistic eigenvalue sensitivity analysis and PSS design in multimachine systems. in <u>IEEE Transactions on Power Systems</u> 18, 4(Nov 2003) : 1439–1445.

[17] Ilea, V., Berizzi, A., and Eremia, M., Damping Inter-area Oscillations by FACTS Devices. in <u>International Universities Power Engineering Conference (UPEC 2009)</u>,pp. 1–5, Sept 2009.

[18] Huang, Z., et al., Use of Modal Sensitivity to Operating Conditions for Damping Control in Power Systems . in <u>2011 44th Hawaii International Conference on System Sciences (HICSS)</u>,pp. 1–9, Jan 2011.

[19] Trudnowski, D.J., et al., Performance of Three Mode-Meter Block-Processing Algorithms for Automated Dynamic Stability Assessment. in <u>IEEE Transactions on Power Systems</u> 23, 2(May 2008) : 680–690.

[20] Hauer, J.F., Demeure, C.J., and Scharf, L.L., Initial results in Prony analysis of power system response signals. in <u>IEEE Transactions on Power Systems</u> 5, 1(Feb 1990) : 80–89.

[21] Pierre, D.A.,Trudnowski, D.J., and Hauer, J.F., Identifying linear reduced-order models for systems with arbitrary initial conditions using Prony signal analysis. in <u>IEEE Transactions on Automatic control</u> 37, 6(Jun 1992) : 831–835.

[22] Sanchez-Gasca, J.J., and Chow, J.H., Computation of power system low-order models from time domain simulations using a Hankel matrix. in <u>IEEE Transactions on Power System</u> 12, 4(Nov 1997) : 1461–1467.

[23] Guoping, L., Quintero, J., and Venkatasubramanian, V., Oscillation monitoring system based on wide area synchrophasors in power systems. in <u>Revitalizing Operational Reliability, 2007 iREP Symposium Bulk Power System Dynamics and Control–VII</u>,pp. 1–13, Aug 2007.

[24] Pierre, J.W.,Trudnowski, D.J.,and Donnelly, M.K., Initial results in electromechanical mode identification from ambient data. in <u>IEEE Transactions on Power System</u> 12, 3(Aug 1997) : 1245–1241.

[25] Wies, R.W., Pierre, J.W., and Trudnowski, D.J., Use of ARMA block processing for estimating stationary low-frequency electromechanical modes of power systems. in <u>IEEE Transactions on Power System</u> 18, 1(Feb 2003) : 167–173.

[26] Zhou, N., Pierre, J., and Wies. R., Estimation of low-frequency electromechanical modes of power systems from ambient measurements using a subspace method. in <u>in Proceedings of the North American Power Symposium</u>, 2003.

[27] Guoping, L., and Venkatasubramanian, V., Oscillation monitoring from ambient PMU measurements by Frequency Domain Decomposition. in <u>IEEE International Symposium on Circuits and Systems, 2008. ISCAS 2008</u>,pp. 2821–2824 , May 2008.

[28] Darren McCrank, P.E., <u>Phasor Measurement Unit Requirement. Alberta Electric System Operator</u>, [online]. 2010. Available from : http://www.aeso.ca/rulesprocedures/9060.html [2013, February 17]

[29] Ouadi, A., Bentarzi, H., Maun, J.C., A new computer based Phasor Measurement Unit framework. in <u>The 6th International Multi-Conference on Systems, Signals and Devices, 2009. SSD '09</u>,pp. 1–6, March 2009.

[30] Missout, G., Girard, P., Measurement of Bus Voltage Angle Between Montreal and SEPT-ILES. in <u>IEEE Transactions on Power Apparatus and Systems</u> PAS–99, 2(March 1980) : 536–539.

[31] Missout, G., Beland,J., and Bedard, G., Dynamic measurement of the absolute voltage angle on long transmission Lines. in <u>IEEE Transactions on Power Apparatus and Systems</u> PAS–100, 11(November 1981) : 4428–4434.

[32] Bonanomi,P., Phase angle measurements with synchronized clocks principles and applications. in <u>IEEE Transactions on Power Apparatus and Systems</u> PAS–100, 11(November 1981) : 5036–5043.

[33] Phadke, A.G., Hlibka, T., and Ibrahim, M., Fundamental basis for distance relaying with symmetrical components. in <u>IEEE Transactions on Power Apparatus and Systems</u> PAS–96, 2(March 1977) : 635–646.

[34] Phadke, A.G., Thorp, J.S, and Adamiak,M.G., A new measurement technique for tracking voltage phasors, local system frequency, and rate of change of frequency. in <u>IEEE Transactions on Power Apparatus and Systems</u> PAS–102, 5(May 1983) : 1025–1038.

[35] Power System Relaying Society: IEEE Power Engineering, <u>C37.118–2005–IEEE Standard for Synchrophasors for Power Systems</u>, [online]. Available at http://ieeexplore.ieee.org/servlet/opac?punumber=10719 [2013, Feb 17]

[36] Li, C., et al., Monitoring and estimation of interarea power oscillation mode based on application of CampusWAMS. in <u>Proceeding CD of 16th Power System Computation Conference, Glasgow</u>, 2008.

[37] Ning, Z., Trudnowski, D., and Pierre, J.W., Mode initialization for on-line estimation of power system electromechanical modes. in <u>Power Systems Conference and Exposition, 2009. PSCE '09. IEEE/PES</u>,pp. 1–8, March 2009.

[38] PNNL, <u>Monitoring grid stability in real-time</u>, [online]. Available at http://eioc.pnnl.gov/research/gridstability.stm. [2013, Feb 17].

[39] Ali, H. R., and Hoonchareon, H., Selection of Phasor Measurement Unit Location for Inter-Area Power Oscillation Identification. in <u>The 5th AUN/SEED-Net Regional Conference in Electrical and Electronics Engineering</u>,pp. 251–254, Feb 2013.

[40] mathworks, <u>Matlab GUI</u>, [online]. Available at http://www.mathworks.com/discovery/matlab-gui.html. [2013, Feb 21].

[41] Chow, J.H., and Cheung, K.W., A toolbox for power system dynamics and control engineering education and research. in <u>IEEE Transactions on Power System</u> 7, 4(Nov 1992) : 1559–1564.

APPENDIX

POWER FLOW AND DYNAMIC DATA OF SIMPLIFIED WNAPS 17 MACHINE SYSTEM

Table A.1: Bus data for simplified WNAPS 17 machine system

Bus	V magnitude	V angle	Pgen	Qgen	Pload	Qload	G	B	type	Qmax	Qmin	Vrate	vmax	vmin
1	1.049	0	20	13	0	0	0	0	1	25	-10	20	1.1	0.9
2	1.049	0	27	20.1	0	0	0	0	2	45	-10	20	1.1	0.9
3	1.049	0	54	38.5	0	0	0	0	2	54	-10	20	1.1	0.9
4	1.049	0	49	33.5	0	0	0	0	2	49	-10	20	1.1	0.9
5	1.049	0	30.5	23	0	0	0	0	2	30.5	-10	20	1.1	0.9
6	1.049	0	45	12.5	0	0	0	0	2	45	-10	20	1.1	0.9
7	1.049	0	17	12.5	0	0	0	0	2	17	-10	20	1.1	0.9
8	1.049	0	26	20	0	0	0	0	2	26	-10	20	1.1	0.9
9	1.049	0	20	13	0	0	0	0	2	25	-10	20	1.1	0.9
10	1.049	0	45.5	33.5	0	0	0	0	2	45	-10	20	1.1	0.9
11	1.049	0	54	38.5	0	0	0	0	2	54	-10	20	1.1	0.9
12	1.049	0	49	33.5	0	0	0	0	2	49	-10	20	1.1	0.9
13	1.049	0	30	23	0	0	0	0	2	30.5	-10	20	1.1	0.9
14	1.049	0	45	12.5	0	0	0	0	2	45	-10	20	1.1	0.9
15	1.049	0	17	12.5	0	0	0	0	2	17	-10	20	1.1	0.9
16	1.049	0	26	20	0	0	0	0	2	26	-10	20	1.1	0.9
17	1.049	0	0	0	0	0	0	25	3	0	0	500	1.5	0.8
18	1.049	0	0	0	0	0	0	10	3	0	0	500	1.5	0.8
19	1.049	0	0	0	0	0	0	0	3	0	0	500	1.5	0.5

Bus	V magnitude	V angle	Pgen	Qgen	Pload	Qload	G	B	type	Qmax	Qmin	Vrate	vmax	vmin
20	1.049	0	0	0	0	0	0	0	3	0	0	500	1.5	0.5
21	1.049	0	0	0	0	0	0	5	3	0	0	500	1.5	0.5
22	1.049	0	0	0	0	0	0	10	3	0	0	500	1.5	0.5
23	1.049	0	0	0	0	0	0	5	3	0	0	500	1.5	0.5
24	1.049	0	0	0	0	0	0	0	3	0	0	230	1.5	0.5
25	1.049	0	0	0	0	0	0	0	3	0	0	500	1.5	0.5
26	1.049	0	0	0	0	0	0	0	3	0	0	500	1.5	0.5
27	1.049	0	0	0	0	0	0	0	3	0	0	230	1.5	0.5
28	1.049	0	0	0	0	0	0	0	3	0	0	230	1.5	0.5
29	1.049	0	0	0	0	0	0	0	3	0	0	230	1.5	0.5
30	1.049	0	0	0	0	0	0	0	3	0	0	230	1.5	0.5
31	1.049	0	0	0	14	4	0	0	3	0	0	230	1.5	0.5
32	1.049	0	0	0	20	12	0	0	3	0	0	230	1.5	0.5
33	1.049	0	0	0	30	12	0	0	3	0	0	230	1.5	0.5
34	1.049	0	0	0	70	30	0	8	3	0	0	230	1.5	0.5
35	1.049	0	0	0	45	21	0	20	3	0	0	230	1.5	0.5
36	1.049	0	0	0	82	40	0	30	3	0	0	230	1.5	0.5
37	1.049	0	0	0	62	28	0	35	3	0	0	230	1.5	0.5
38	1.049	0	0	0	55	25	0	20	3	0	0	230	1.5	0.5
39	1.049	0	0	0	54	20	0	7	3	0	0	230	1.5	0.5
40	1.049	0	0	0	44	26	0	15	3	0	0	230	1.5	0.5
41	1.049	0	0	0	54	26	0	15	3	0	0	230	1.5	0.5
42	1.049	0	0	0	10	0	0	0	3	0	0	110	1.5	0.5
43	1.049	0	0	0	-10	0	0	0	3	0	0	110	1.5	0.5

Bus	V magnitude	V angle	Pgen	Qgen	Pload	Qload	G	B	type	Qmax	Qmin	Vrate	vmax	vmin
45	1.0483	0	0	0	0	0	0	0	3	0	0	500	1.5	0.5

Table A.2: Lines data for simplified WNAPS 17 machine system

from bus	to bus	resistance(pu)	reactance(pu)	line charging(pu)	tap ratio	tap phase	tap max	tap min	tap size
1	17	0	0.0018	0	1	0	0	0	0
2	18	0	0.0007	0	1	0	0	0	0
3	19	0	0.0006	0	1	0	0	0	0
4	20	0	0.0007	0	1	0	0	0	0
5	21	0	0.0011	0	1	0	0	0	0
6	22	0	0.0006	0	1	0	0	0	0
7	23	0	0.0019	0	1	0	0	0	0
8	24	0	0.0013	0	1	0	0	0	0
9	17	0	0.0018	0	1	0	0	0	0
10	18	0	0.0007	0	1	0	0	0	0
11	19	0	0.0006	0	1	0	0	0	0
12	20	0	0.0007	0	1	0	0	0	0
13	21	0	0.0011	0	1	0	0	0	0
14	22	0	0.0006	0	1	0	0	0	0
15	23	0	0.0019	0	1	0	0	0	0
16	24	0	0.0013	0	1	0	0	0	0
17	34	0.0076	0.084	0.88	0	0	0	0	0
34	18	0	0.005	0.05	0	0	0	0	0
34	18	0	0.005	0.05	0	0	0	0	0

from bus	to bus	resistance(pu)	reactance(pu)	line charging(pu)	tap ratio	tap phase	tap max	tap min	tap size
18	30	0.002533	0.028	0.2933	0	0	0	0	0
17	30	0	0.001	0	0	0	0	0	0
17	35	0.00075	0.0047	0.0045	0	0	0	0	0
17	35	0.00075	0.0047	0.0045	0	0	0	0	0
35	21	0.00225	0.0141	0.0135	0	0	0	0	0
17	32	0.0000775	0.000875	0.005625	0	0	0	0	0
32	22	0.0002325	0.002625	0.016875	0	0	0	0	0
17	33	0.0002775	0.00261	0.00825	0	0	0	0	0
33	22	0.0000925	0.00087	0.00275	0	0	0	0	0
19	37	0.0004	0.0031	0.0064	0	0	0	0	0
37	20	0.0016	0.0124	0.0256	0	0	0	0	0
19	29	0	0.005	0	1	0	0	0	0
20	25	0.0001	0.00075	0.04	0	0	0	0	0
20	38	0	0.0015	0	1	0	0	0	0
21	36	0.00126	0.008856	0.0584	0	0	0	0	0
21	36	0.00126	0.008856	0.0584	0	0	0	0	0
21	36	0.00126	0.008856	0.0584	0	0	0	0	0
36	25	0.0224	0.1575	0.5544	0	0	0	0	0
21	36	0.001575	0.01107	0.1	0	0	0	0	0
36	26	0.0032	0.0225	0.0792	0	0	0	0	0
22	31	0.00095	0.00775	0.0476	0	0	0	0	0
22	45	0.004	0.04	0.4	0	0	0	0	0
23	31	0.00095	0.00775	0.0476	0	0	0	0	0
22	27	0	0.007	0	1	0	0	0	0

from bus	to bus	resistance(pu)	reactance(pu)	line charging(pu)	tap ratio	tap phase	tap max	tap min	tap size
23	28	0	0.007	0	1	0	0	0	0
24	39	0	0.0015	0	1	0	0	0	0
24	27	0.008	0.084	0.334	0	0	0	0	0
24	28	0.0085	0.0995	0.5	0	0	0	0	0
24	29	0.0092	0.109	0.5	0	0	0	0	0
25	26	0	0.00005	0	0	0	0	0	0
25	40	0	0.0015	0	1	0	0	0	0
26	41	0	0.0015	0	1	0	0	0	0
44	45	0	0.001	0	1	0	0	0	0
17	42	0	0.01	0	1	0	1.5	0.5	0.005
26	43	0	0.01	0	1	0	1.5	0.5	0.005

Table A.3: Machines data for simplified WNAPS 17 machine system

Machines no	bus	base	x_l	r_a	x_d	$x_d^{'}$	$x_d^{"}$	$T_{do}^{'}$	$T_{do}^{"}$	x_q	$x_q^{'}$	$x_q^{"}$	$T_{qo}^{'}$	$T_{qo}^{"}$	H	d_0
1	1	2750	0	0	0.9	0.27	0	9	0	0.6	0.27	0	0.05	0	4.4	1
2	2	7000	0	0	0.9	0.27	0	9	0	0.6	0.27	0	0.05	0	4.6	1.5
3	3	8000	0	0	1.7	0.27	0	6	0	1.6	0.27	0	0.8	0	4	1
4	4	7000	0	0	1.7	0.27	0	6	0	1.6	0.27	0	0.8	0	4.8	1
5	5	4750	0	0	1.7	0.27	0	6	0	1.6	0.27	0	0.8	0	4.9	1.5
6	6	8000	0	0	0.9	0.27	0	9	0	0.6	0.27	0	0.05	0	5	1.5
7	7	2600	0	0	1.7	0.27	0	6	0	1.6	0.27	0	0.8	0	3.3	1
8	8	4000	0	0	0.9	0.27	0	9	0	0.6	0.27	0	0.05	0	2.8	0.5

Machines no	bus	base	x_l	r_a	x_d	$x_d^{'}$	$x_d^{''}$	$T_{do}^{'}$	$T_{do}^{''}$	x_q	$x_q^{'}$	$x_q^{''}$	$T_{qo}^{'}$	$T_{qo}^{''}$	H	d_0
9	9	2750	0	0	0.9	0.27	0	9	0	0.6	0.27	0	0.05	0	4.4	1
10	10	7000	0	0	0.9	0.27	0	9	0	0.6	0.27	0	0.05	0	4.6	1.5
11	11	8000	0	0	1.7	0.27	0	6	0	1.6	0.27	0	0.8	0	4	1
12	12	7000	0	0	1.7	0.27	0	6	0	1.6	0.27	0	0.8	0	4.8	1
13	13	4750	0	0	1.7	0.27	0	6	0	1.6	0.27	0	0.8	0	5.9	1.5
14	14	8000	0	0	0.9	0.27	0	9	0	0.6	0.27	0	0.05	0	5	1.5
15	15	2600	0	0	1.7	0.27	0	6	0	1.6	0.27	0	0.8	0	3.3	1
16	16	4000	0	0	0.9	0.27	0	9	0	0.6	0.27	0	0.05	0	2.8	0.5
17	44	18000	0	0	0.9	0.27	0	9	0	0.6	0.27	0	0.05	0	5	1.5

Table A.4: Excitation data for simplified WNAPS 17 machine system

Type	machine	T_R	K_A	T_A	T_B	T_C	$Vmax$	$Vmin$
Simple exciter	1	0	200	0.04	12	1	6	-3
Simple exciter	2	0	200	0.04	12	1	6	-3
Simple exciter	3	0	250	0.03	12	1	7	-2
Simple exciter	4	0	200	0.04	12	1	6	-3
Simple exciter	5	0	250	0.03	12	1	7	-2
Simple exciter	6	0	200	0.04	12	1	6	-3
Simple exciter	7	0	200	0.04	12	1	6	-3
Simple exciter	8	0	200	0.04	12	1	6	-3
Simple exciter	9	0	200	0.04	12	1	6	-3
Simple exciter	10	0	200	0.04	12	1	6	-3

Type	machine	T_R	K_A	T_A	T_B	T_C	$Vmax$	$Vmin$
Simple exciter	11	0	250	0.03	12	1	7	-2
Simple exciter	12	0	200	0.04	12	1	6	-3
Simple exciter	13	0	200	0.03	12	1	7	-2
Simple exciter	14	0	200	0.04	12	1	6	-3
Simple exciter	15	0	200	0.04	12	1	6	-3
Simple exciter	16	0	200	0.04	12	1	6	-3
Simple exciter	17	0	200	0.04	12	1	6	-3

Table A.5: PSS data for simplified WNAPS 17 machine system

Input	machine	K	Tw	T1	T2	T3	T4	max	min
Speed	1	20	10	0.2	0.02	0.4	0.04	0.1	-0.1
Speed	2	20	10	0.2	0.02	0.4	0.04	0.1	-0.1
Speed	3	20	10	0.2	0.02	0.2	0.02	0.1	-0.1
Speed	4	20	10	0.2	0.02	0.2	0.02	0.1	-0.1
Speed	5	20	10	0.2	0.02	0.2	0.02	0.1	-0.1
Speed	6	20	10	0.2	0.02	0.4	0.04	0.1	-0.1
Speed	7	20	10	0.2	0.02	0.4	0.04	0.1	-0.1
Speed	8	20	10	0.2	0.02	0.4	0.04	0.1	-0.1
Speed	9	20	10	0.2	0.02	0.4	0.04	0.1	-0.1
Speed	10	20	10	0.2	0.02	0.4	0.04	0.1	-0.1
Speed	11	20	10	0.2	0.02	0.2	0.02	0.1	-0.1
Speed	12	20	10	0.2	0.02	0.2	0.02	0.1	-0.1
Speed	13	20	10	0.2	0.02	0.2	0.02	0.1	-0.1

Input	machine	K	Tw	T1	T2	T3	T4	max	min
Speed	14	20	10	0.2	0.02	0.4	0.04	0.1	-0.1
Speed	15	20	10	0.2	0.02	0.4	0.04	0.1	-0.1
Speed	16	20	10	0.2	0.02	0.4	0.04	0.1	-0.1
Speed	17	20	10	0.2	0.02	0.4	0.04	0.1	-0.1

Table A.6: Governor data for simplified WNAPS 17 machine system

machine	speed set point	$1/R$	Tmax	Ts	Tc	T3	T4	T5
9	1	20	1	0.4	75	10	-2.4	1.2
10	1	20	1	0.4	75	10	-2.4	1.2
11	1	20	1	0.04	0.2	0	1.5	5
12	1	20	1	0.04	0.2	0	1.5	5
13	1	20	1	0.04	0.2	0	1.5	5
14	1	20	1	0.4	75	10	-2.4	1.2
15	1	20	1	0.04	0.2	0	1.5	5
16	1	20	1	0.4	75	10	-2.4	1.2

Biography

Husni Rois Ali was born in Yogyakarta, Indonesia, in 1987. He received his B.Eng in electrical engineering from Gadjah Mada University (UGM), Indonesia, in 2009. In the same year, he joined Department of Electrical Engineering as a teaching staff. Since 2011, He pursue his M.Eng. at Department of Electrical Engineering, Chulalongkorn University, Thailand under the support from AUN/SEED-Net (www.seed-net.org). His main research interest is on power system dynamic, stability, and control.

List of Publications

1. Ali, H., R., and Hoonchareon, N., Application of Prony Analysis to Identification of Low Frequency Power Oscillation. in *Proc. of EECON-35 conference*. (2012).

2. Ali, H., R., and Hoonchareon, N., Selection of Phasor Measurement Unit Location for Inter-Area Power Oscillation Identification. in *Proc. of the 5th AUN/SEED-Net Regional Conference in Electrical and Electronic Engineering*. (2013).

3. Ali, H., R., and Hoonchareon, N., Real-Time Monitoring of Inter-Area Power Oscillation Using Phasor Measurement Unit, *Proc. of ECTI-CON*. (2013).